Energy 266 (2023) 126317

Contents lists available at ScienceDirect

Energy

journal homepage: www.elsevier.com/locate/energy

Evaluating the use of a Net-Metering mechanism in microgrids to reduce power generation costs with a swarm-intelligent algorithm

C.G. Marcelino [a,b,*], G.M.C. Leite [b,c], E.F. Wanner [d], S. Jiménez-Fernández [b], S. Salcedo-Sanz [b,e]

[a] Institute of Computing, Federal University of Rio de Janeiro (UFRJ), Brazil
[b] Department of Signal Processing and Communications, Universidad de Alcalá, Spain
[c] Systems and Computing Department, Federal University of Rio de Janeiro, Brazil
[d] Computing Department, Federal Center of Technology Education of MG, Brazil
[e] USQ's Advanced Data Analytics Lab, School of Mathematics, Physics and Computing, University of Southern Queensland, Springfield, QLD, 4300, Australia

ARTICLE INFO

Keywords:
Microgrid systems
Net-Metering
Renewable sources
Swarm evolutionary optimization

ABSTRACT

The micro-generation of electricity arises as a clean and efficient alternative to provide electrical power. However, the unpredictability of wind and solar radiation poses a challenge to attend load demand, while maintaining a stable operation of the microgrids (MGs). This paper proposes the modeling and optimization, using a swarm-intelligent algorithm, of a hybrid MG system (HMGS) with a Net-Metering compensation policy. Using real industrial and residential data from a Spanish region, a HMGS with a generic ESS is used to analyze the influence of four different Net-Metering compensation levels regarding costs, percentage of renewable energy sources (RESs), and LOLP. Furthermore, the performance of two ESSs, Lithium Titanate Spinel ($Li4Ti5O_{12}$ (LTO)) and Vanadium redox flow batteries (VRFB), is assessed in terms of the final $/kWh costs provided by the MG. The results obtained indicate that the Net-Metering policy reduces the surplus from over 14% to less than 0.5% and increases RESs participation in the MG by more than 10%. Results also show that, in a yearly projection, a MG using a VRFB system with a 25% compensation policy can yield more than 100000$ dollars of savings, when compared to a MG using a LTO system without Net-Metering.

1. Introduction

In the European Union (EU) context, the share of energy from renewable sources in the gross final consumption of energy increased by 17% in 2016, doubling the share in 2004 (8.5%). The 2020 European strategy included a target of reaching 20% of energy in the gross final consumption of energy from renewable sources by 2020. This target was met with the EU achieving 22.1% by the end of 2020. Following this increase, the target for 2030 is set to 32%. These figures are based on energy use in all its forms across all three main sectors, the heating and cooling sector, the electricity sector, and the transport sector [1,2]. To achieve the future targets for the transition towards climate neutrality, EU countries need to prioritize more effectively the deployment of renewable energy sources and invest in improving energy efficiency.

These goals are based on the fact of the growing and exponential demand for energy, caused by the impact of the imminent depletion of fossil fuels and the environmental impact they cause. In this context, the addition of microgrid generation (MG) systems has attracted the attention of European countries in the electrical sector. The use of clean and sustainable generation becomes a promising bet for the generation of electricity on a global scale [3–5].

MG comprises low-voltage distribution systems with distributed energy resources (microturbines, fuel generators, photovoltaic panels, among others) along with storage devices (energy capacitors and energy storage systems), and flexible loads. These systems can be operated autonomously in a standalone way, or non-autonomously, interconnected to the main grid — in a grid-connected approach. Operating MG on the public grid can provide important benefits for overall system performance if managed and coordinated efficiently [6,7].

The general benefits of generating electricity via MG include: allowing access to electricity in remote regions [8,9] and minimizing both the generation costs [10,11] and carbon emissions [12–14]. However, generating electricity via renewable sources has some challenges: the lack of regulation that standardizes the generation and integration of the generated energy into the public grid [15]. Developments in renewable electricity generation, distribution, and storage are constantly in need to achieve the goal of changing energy production into a mainly renewable-based one.

* Corresponding author at: Institute of Computing, Federal University of Rio de Janeiro (UFRJ), Brazil.
E-mail addresses: carolina@ic.ufrj.br (C.G. Marcelino), gmatos@cos.ufrj.br (G.M.C. Leite), efwanner@cefetmg.br (E.F. Wanner), silvia.jimenez@uah.es (S. Jiménez-Fernández), sancho.salcedo@uah.es (S. Salcedo-Sanz).

https://doi.org/10.1016/j.energy.2022.126317
Received 10 August 2022; Received in revised form 1 November 2022; Accepted 30 November 2022
Available online 8 December 2022
0360-5442/

The net-Metering policy is a utility billing mechanism that allows residential or commercial users who generate their own electricity (using solar panels or photovoltaic systems) to send back to the grid their surplus energy. This mechanism has many advantages such as providing extra financial credit, eliminating the need for battery storage and backup generator, and being inexpensive, among others. The Net-Metering mechanism is vital for the goals of future power systems [16], and is being adopted worldwide [17]. From the producer–consumers (prosumers) point of view, besides the subsidy from the government, the offering of a net-metering policy by the Distribution Companies can be very attractive in reducing the prices of photovoltaic (PV) panels, as pointed out in [18]. The study presented in [19] shows that, when the Net-Metering policy does not provide much compensation to the end user, the prosumers tend to forego investing in renewable sources. In Brazil, for example, in order to attract prosumers to adopt renewable energy generators, a law issued by the government regulates the compensation policy for users that opt to connect to the grid. This law states that the power injected by each user remains valid for a period of 60 months and can be compensated in an address different from the one that the power was injected [20–23]. However, such policies must be aligned with the distribution companies' interests. As indicated in [24], as the penetration of renewable generation in the MG increases, the Net-Metering policy must be carefully analyzed. A Net-Metering policy that only benefits the end user by compensating injected energy at the retail price may lead to a reduction in the companies' revenues.

1.1. Literature review

Several recent works have studied the inclusion and optimization of different procedures and technologies in MGs, such as the Net-Metering procedure, diverse control mechanisms, and different energy storage systems (ESS) technologies. We revise here the recent literature works on these topics. In [25] the effectiveness of China's Net-Metering subsidies for household distributed photovoltaic systems is assessed. [26] showed alternatives for current Net-Metering in the Netherlands: a comparison of impacts on a business case and purchasing behavior of private homeowners, and on governmental costs. Australian's government policy towards energy has been dominated by an array of interventions and market-based instruments [27]. A study carried out in Italy showed the advantage to prosumers in performing Net-Metering. According to [17], the use of Net-metering system has been recently adopted in many countries such as Italy [16], USA [28], and Brazil [22]. However, other countries, such as Spain, are still facing the market and institutional barriers to the use of the mechanism in the public power grid [29,30].

Numerous approaches to provide control mechanisms in MGs, especially in grid-connected mode, to ensure a reliable and sustainable operation have been addressed in the literature. [7,31] bring forward two surveys describing thirty works that include approaches for optimal control of MG applied to different countries. In addition to these works, the recent literature discusses different optimization techniques applied to a diverse range of MG systems. A study applied to the region of Bangladesh analyzing how it is possible to optimize load dispatch strategies was carried out in [32]. Using the Simulink tool, the results showed that the techno-economic feasibility and system stability responses (voltage and frequency) were achieved via the default optimization tools in MATLAB. A deep learning method based on Convolutional Neural Networks is proposed in [33] to develop a wake model for wind turbines in real-time. The obtained model is evaluated in a wind farm containing 25 wind turbines, obtaining minimal error to predict the dynamic wind farm wakes with respect to wind speed. Aiming at achieving higher wind speeds, [34] proposed an optimization tool to optimize the design parameters for a specific geometry of floating offshore wind turbines. The results showed that the optimal design obtained reduces cost by two to three times the worst cost scenario.

A mixed integer linear programming (MILP) approach was proposed by [35,36] to solve the coordinated control in a dynamic optimization way in direct current power in microgrid systems. The simulation indicated that the control system showed a fast recovery and robust performance from the transient using the mode-override operation of storage systems, thus coordinating with generators. [37,38] proposed a dispatch controller via robust optimization. [39] developed a solution to find the optimal size of a microgrid system using the Grasshopper optimization algorithm (GOA). The results indicated that GOA was able to optimally size the system as compared to Particle Swarm Optimization. GOA, in a multi-objective approach, was able to minimize the production costs and the CO2 emissions of a simulated microgrid [40].

The sector of new technologies in EES has been drawing attention and is in a constant expansion [41,42]. In general, the lithium-ion (Li-ion) battery class have a high cost per power capacity and high energy density [43]. On the other hand, batteries based on redox flow have some innovative features such as design flexibility and greater cycle capacity, even though they still have a high-cost [44]. In this work, we investigate two potential technologies to identify which one is best suited to the studied MG, named the lithium titanate spinel ($Li4Ti5O_{12}$ (LTO) – [45]) and Vanadium redox flow (VRFB – [46]).

Regarding the benefits of using Energy Storage Systems (ESSs) in a microgrid, it is worth noting the reduction in the system peak and congestion [47] and the leveling of the load [48]. In [49] a cost–benefit analysis for load leveling is proposed, in which a Li-ion battery is compared to a RFVB in terms of return on investment and cost savings. The results indicated that the Li-ion battery is superior to the RFVB in both comparisons. Similarly, a techno-economic analysis considering a commercial building is made in [50]. In this analysis, a Li-ion battery is compared to two other batteries that use reversible fuel cells by means of Levelized Cost Of energy Storage (LCOS) with and without considering ESS's degradation. As a result, despite being prone to degradation, Li-ion batteries are economically attractive. Contrarily, as wisely pointed out by [51], despite the high cost and longer life cycle, VRFBs produce less environmental impact than Li-ion batteries. The environmental advantages of RFVBs are also assessed by [52] in a combination with a hydropower plant in Ecuador. The ESS is used to inject energy into the main grid during peak hours.

With respect to combining multiple ESSs, [53] solved an ESS control problem by integrating the uncertainties of renewable energy sources generation into the problem and minimizing the use of ESSs to correct forecast errors. The targeted control problem is solved using Stochastic Model Predictive Control techniques and Mixed-Integer Quadratic Programming. [54] proposed an Alternating Direction Method of Multipliers (ADMM) to minimize the costs of a system containing multiple microgrids and a combination between BESS and a thermal energy storage system.

Diverse bio-inspired algorithms were addressed in [55]. The results showed that such algorithms are suitable to manage and provide electric control of MG successfully. The genetic algorithm (GA) applied to managing MG systems was described in [56], [57]. Results showed that the performances are just 10% below when compared to the fuzzy-systems approach. [58,59] proposed an optimal energy management and control aspects using multi-agent systems. In general, approaches via multi-agent systems have a high computational cost, which makes their application in a real system unfeasible. Particle Swarm Optimization (PSO) was applied to reduce the operational cost for a hybrid residential standalone microgrid consisting of a diesel generator, wind turbines (WT), photovoltaic (PV) panels and battery energy storage systems [60]. The experiments addressed that the use of storage systems minimized fuel consumption, and therefore the CO2 emission was the lowest. Maintaining State-of-Charge (SoC) in batteries is also an important topic in the study of microgrid systems. For instance, PSO was well applied by [61] as a control system able to choose the optimal

generation source, minimizing the material and financial costs. In [62] PSO is also applied to develop a fuzzy logic controller to manage the charge and discharge of the BESS in a MG. The MG addressed in the aforementioned problem contained a diesel generator, a PV system, WTs, and biomass.

A version of the Multi-Objective Particle Swarm Optimization (MOPSO) algorithm was used in [63–65] to provide control while ensuring the maximum utilization of generation sources and maintaining SoC to manage the exchange of power between the MG studied. A Differential Evolution (DE) application can be observed in [66–68]. In general, the DE quickly converged attaining feasible and efficient solutions.

1.2. Contributions

To the best of our knowledge, the algorithms and approaches described before have not yet been applied to construct an optimization solution based on the Net-Metering mechanism. In this paper we propose to incorporate and optimize the Net-Metering mechanism into a MG, taking into account the seasonal and load data from a Spanish region. Two distinct storage technologies, VRFB and LTO, are assessed and compared in an annual planning horizon. For optimizing the proposed MG, the C-DEEPSO algorithm [69] is employed. C-DEEPSO is a single-objective swarm optimization method with selection and self-adaptive properties inspired by Differential Evolution. The rationale behind this choice is due to its ease of implementation, fast convergence, and efficiency in finding good solutions to electrical dispatch problems in MG. In this case, C-DEEPSO acts as an electrical dispatch controller system, capable of offering optimized solutions for the annual planning horizon. The paper presents the following contributions:

- An improved mathematical modeling to electric dispatch including the Net-Metering policy;
- A study on the effectiveness of the Net-Metering approach applied to a Spanish scenario;
- An in-depth performance assessment of two distinct storage systems, named VRFB and LTO in the MG, and;
- A projection analysis has been carried out indicating a profit economy when solving the problem using the proposed approach.

The remainder of this paper has been organized as follows: Section 2 describes the MG system considered, detailing the electrical dispatch mathematical modeling, the Net-Metering mechanism, and the seasonal and technical data. Section 3 addresses the optimization technique used to solve the electric dispatch problem introducing the fundamentals of the C-DEEPSO method. Section 4 comprises the experimental design performed, and the comparative analysis of the MG system with and without Net-Metering mechanism. After that, a study of which storage system is the most suitable to the MG and a techno-economic analysis are done Finally, Section 5 illustrates the conclusions regarding the overall compensation policy robustness.

2. Microgrid systems

Currently, with the challenges of energy decentralization and the automation of systems, proposing new solutions for grid-connected MG has become an emerging economic development and research area. A power dispatch problem defined in MG tries to find the optimal scheduling for the MG, aiming to meet the load demand while satisfying all systems constraints. The mathematical model of the proposed MG and the considered optimization problem are described next.

2.1. Power dispatch problem: mathematical modeling in microgrids

This work addresses the optimal active power dispatch problem in MGs, with the goal of minimizing the total costs of production and losses in the system. The MG addressed here is composed of photovoltaic panels (PV), micro wind turbines (WT), energy storage system (ESS), AC–DC inverter (INV), and energy from the public grid system (PG). In this context, the power generated by PV can be obtained by Eq. (1) [70],

$$P_{pv} = P_N \times \frac{G}{G_{ref}} \times \left[1 + K_t \left((T_{amb} + (0.0256 \times G)) - T_{ref}\right)\right], \tag{1}$$

in which P_{pv} is the power production of PV's (in kW/h) and P_N is rated power under reference conditions. The term G means the solar radiation (W/m^2), G_{ref} is a constant equals to 1000 (W/m^2), T_{ref} is the average temperature in Cádiz (Spain) equals to 18 °C, K_t it is a constant equals to -3.7×10^{-3} (1/°C), and T_{amb} is the ambient temperature [70].

The power wind production depends on wind variation. Thus, the power law equation to wind turbines is calculated by the following correlation: $\frac{v_2}{v_1} = \left(\frac{h_2}{h_1}\right)^{\alpha}$ [71]. The wind gradient (α) is a function of parameters such as wind speed, temperature, hour of the day, time of the year, the roughness of the terrain, and the height above ground [71]. Usually, we can use $\alpha = 1/7$ [70]. The term v_2 is the speed at the hub height (h_2) and v_1 is the speed at the reference height (h_1). Following these rules, the power output of wind turbine can be approximated by [71]:

$$P_w = \begin{cases} 0 & V < V_{cut-in}, V > V_{cut-out} \\ P_r \left(\frac{V^3 - V^3_{cut-in}}{V^3_r - V^3_{cut-in}}\right) & V_{cut-in} \leqslant V < V_{rated} \\ P_r & V_{rated} \leqslant V \leqslant V_{cut-out} \end{cases} \tag{2}$$

in which, P_r is rated power, V is the wind speed in the current time step. Terms $V_{cut-out}$, V_{rated}, and V_{cut-in} represent cut-in wind speed, nominal wind speed, and cut-out wind speed respectively. The real electric power from the wind generator (in kW/h) can be given by [72]:

$$P_{wind} = P_w \times \eta_w \times A_w, \tag{3}$$

in which η_w is the turbine efficiency and A_w is the total swept area of the wind turbine. An important component in microgrids is the DC/AC converter (inverter). An inverter converts the electrical energy from DC into AC with the desired frequency of the load. The efficiency of the inverter can be defined by the following Eq. (4) [70],

$$\eta_{inv} = \frac{P}{P + P_0 + \kappa \times P^2}. \tag{4}$$

The initial power (P_0), κ, and power (P) are given by [70]

$$P_0 = 1 - 99\left(\frac{10}{\eta_{10}} - \frac{1}{\eta_{100}} - 9\right)^2, \kappa = \frac{1}{\eta_{100}} - P_0 - 1, P = P_{out}/P_n, \tag{5}$$

in which η_{10} and η_{100} are provided by the manufacturers and represent the efficiency of the inverter at 10% and 100% of its nominal power, respectively. Then, the inverter input power is ($P_{inv} = \frac{P_{load}}{\eta_{inv}}$) in which P_{load} is the power consumed by the load and η_{inv} is the inverter efficiency.

The proposed model considers a grid-connected system allowing the wind turbines and photovoltaic cells to be used in synchronized connection with a public grid supply ($P_{grid} = 0.73$ \$h), in case the system does not meet the demand. Here, the EES capacity (in kW) of the system is designed according to the demand and the days of autonomy using the following Eq. (6) [73],

$$c_d = \frac{c_{bat}}{L_c \times E_s \times DoD}. \tag{6}$$

c_d is the degradation cost of ESS, L_c is the degradation in terms of available cycle lifetime, and E_s is the energy storage capacity, at a

certain depth of discharge (DoD) related to the total ESS cell costs (c_{bat}). In our modeling the total cost of installation, maintenance, and operation (C_{total}) can be obtained by Eq. (7) [73]:

$$C_{total} = IC + PW_p + PW_{np} + \sum_{h=1}^{h=8640} c_d, \tag{7}$$

in which the value C_{total} represents the sum of the system initial cost (IC) — personnel cost, installation and connections – periodic costs PW_p — maintenance of PV panels, maintenance of wind generator, among others, and the non-recurrent cost PW_{np} characterized as a cost of ESS replacement and others [73].

2.2. Optimization modeling

A simple approach to simultaneously minimize two or more objective functions is to use a weighted sum of the objectives creating a mono-objective optimization problem [74]. In scalarized approach, the weights of the functions are associated with the importance of each objective. The resulting mono-objective problem is given by:

$$\min f = \left\{ \sum_{i=1}^{k} w_i \frac{f_i(x)}{f_i^{max}} \right\}, \tag{8}$$

$$w_i \geq 0 \text{ and } \sum_{i=1}^{k} w_i = 1$$

$$\text{subject to} : min\ g_i(x) \geq 0\ for\ i \in \{1, \ldots, m\},$$

in which k is the number of objectives. The terms w_i are the weights for each objective, x is the vector of decision variables, f is the objective function and f_i^{max} is the upper bound of ith objective function. Functions $g_i(x)$ are the inequality constraints of problem.

Here, the two functions we want to optimize are the total costs in electricity (COE) and losses of power supply probability (LOLP). COE can be obtained (in $/kWh), by using the following Eq. (9) [73],

$$COE(\$/h) = \frac{C_{total}}{\sum_{h=1}^{h=8640} P_{load}} \times CRF, \tag{9}$$

in which C_{total} means the total costs of installation, maintenance, and operation described in Eq. (7). Power consumption over time (using 24 h × 30 days × 12 months = 8640h) is given by P_{load}. The CRF is a ratio to calculate the present value of the costs for a given planning horizon taking into consideration the interest rate.

Statistical techniques and chronological simulation approaches are used to calculate the LOLP. As a novelty, the modeling proposed the inclusion of two factors in the calculation of LOLP:

1. the power generated by the public grid which, in some situations, may generate exceeding energy. The surplus may be used to charge the ESS. It provides a more environmentally friendly approach, and;
2. the state of charge of the battery. The state of charge of the ESS is a measure of the short-term capacity of the battery and it changes over time since the battery capacity gradually reduces as it ages.

These inclusions provide a more realistic model. For calculating the LOLP, time series data in a given period are based on the energy accumulative effect of ESS as expressed [73],

$$LOLP(\%) = \frac{\sum P_{load} - P_{pv} - P_{wind} + P_{grid} + P_{soc_{min}}}{\sum P_{load}}, \tag{10}$$

in which P_{load} is the hourly power consumption, P_{pv} is the power generated by PV (in kW), P_{wind} is the power (in kW) provide by the wind generator. P_{grid} is the power (in kW) received from public grid and $P_{soc_{min}}$ is the minimum state of charge of the battery (in kW).

An important piece of information is to know how much energy has been generated via renewable sources by the microgrid. Thus, the renewable energy factor (REF) is defined as a boundary to determine the amount of energy coming from the public grid as compared to the renewable sources inside the microgrid. Thus, we use the REF as a constraint problem. When REF is close to 100%, it means that the system is based on renewable resources only. On other hand, when REF is close to zero percent, it shows that the amount of power coming from the public grid is equivalent to the power from renewable resources. REF can be calculated by Eq. (11) [73],

$$REF(\%) = \frac{\sum P_{pv} + P_{wind} + P_{soc_{min}} - P_s}{P_{grid}}, \tag{11}$$

in which P_s stands for the surplus energy amount.

In our modeling, the COE and the LOLP are equally important since the obtained system must guarantee reliability and uninterrupted energy supply at a competitive cost. In this way, the scalarized objective function proposed in this work is described by [73],

$$f = \omega \times LOLP + \omega \times COE + \rho \sum_{i=1}^{n} \max\left[0, REF\right]^2, \tag{12}$$

in which $\omega = 0.5$ is the weight applied to COE and LOLP and ρ is a penalty factor associated with the REF constraint.

2.3. Net-metering

Microgrid systems connected to the main public grid can have meters that, instead of just recording incoming energy flow from the public grid, record both income and outcome energy flows. Incoming energy flow means that the user is using more energy than it is being produced and, outcome energy flow means that the amount of energy produced surpasses the amount consumed. The use of such meters allows the use of an electricity policy, namely Net-Metering, in which users send surplus energy back to the grid whilst receiving compensation in the electricity bill [75,76].

Under a net metering policy, the user can opt to sell either all the renewable energy produced or the excess energy. The compensation mechanism varies depending on the country. For instance, in California - EUA, there are 2 different feed-in tariffs (FiT) distinguishing users that sell excess from users that sell all the electricity generated [77]. Alternatively, in European countries, a common policy is to use the public grid as a backup system for the excess energy production [76,78] in which it is possible to retrieve the energy at zero price or paying a fraction of retail price.

Besides providing financial advantages to customers, net metering policies contribute to improvements in the public grid. The energy sent back to the grid from PV and WT systems can raise the voltage in the grid. This higher voltage helps to prevent temporary blackouts in remote areas, such as rural properties because voltage tends to drop at the end of long distribution lines under high demand. In this way, net metering policies also help to strengthen the grid [79].

In this work, we assume that the net metering policy employed uses the grid as a backup system. We vary the compensation of the backup energy that is retrieved from the grid to 0%, 25%, 50%, and 75% of the retail price. Thus, the P_{grid} factor is split into P_{grid} and P_{met}, in which P_{met} stands for the amount of energy consumed from backup system. Fig. 1 illustrates the HMGS flowchart, in which the orange steps indicate power consumed both from the public grid and backup storage. Furthermore, Eqs. (10) and (11) are modified to include the new parameter as follows,

$$LOLP(\%) = \frac{\sum P_{load} - P_{pv} - P_{wind} + P_{grid} + P_{met} + P_{soc_{min}}}{\sum P_{load}}, \tag{13}$$

$$REF(\%) = \frac{\sum P_{pv} + P_{wind} + P_{soc_{min}} - P_s}{P_{grid} + P_{met}}. \tag{14}$$

It is important to note that the excess energy is sent to the grid only if the battery is fully charged. In other words, PV and WT excess power generated firstly charge the battery and then, if there is any power left, is sold to the grid.

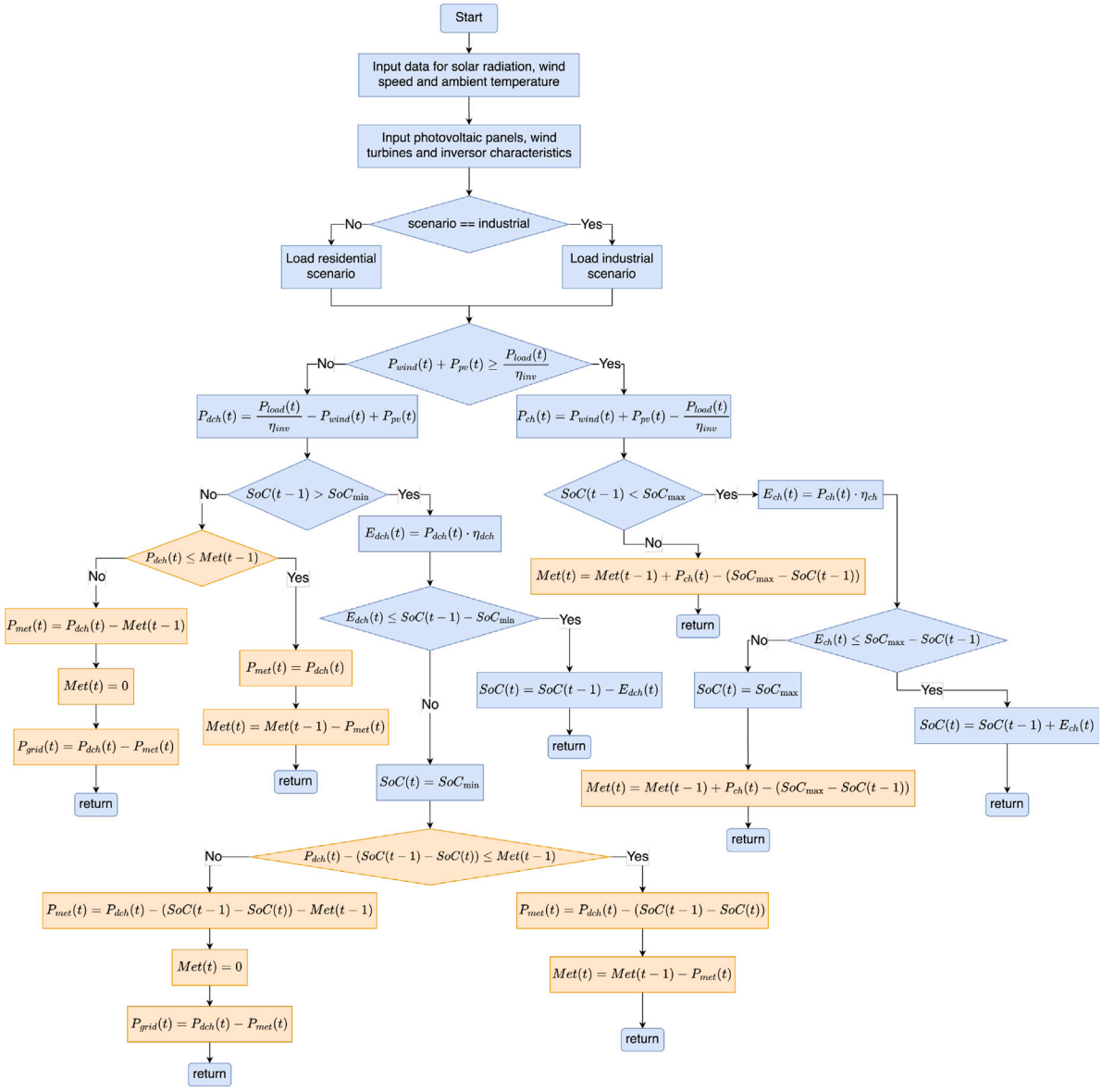

Fig. 1. Flowchart of the modeled HMGS with Net-Metering.

2.4. Technical data information: a case study in Spain

A generic region in Campo de Gibraltar, in Southern Spain, was used as a hypothetical locality for the case study of this work. Seasonal annual series (measured in 8640 h) for typical loads from a residential community and industrial consumption (provided by a Spanish energy company), the series of solar radiation, hourly wind speed, and ambient temperature extracted from a public repository (see [80]) serve as model inputs. Different data series for the period of one year are shown in Fig. 2, in which the data was extracted from [81].

The proposed microgrid has different renewable energy sources. Inverter costs are scale-dependent and based on [82] techno-economic values. Performance curves for small wind turbines are taken from [83], and the other values are taken from [70,83]. The costs and general characteristics of the equipment are described in Table 1. The extra information regarding the WTs specification are: swept area = 113.1 m, cut out = 20 m/s, and cut in = 3 m/s.

As previously described, our approach takes into account energy injection via the public grid. Thus, we consider the electricity end-user price of 0.4892 $/kWh which is the daily electricity average cost in Spain. Some economic parameters are also part of the costs, such as a discount rate of 6%, inflation rate of 1.4%, Operation&Maintenance+ running cost of 20%, and project lifetime of 24 years.

Table 1
General information about INV, PV, and WT. PV is the nominal power. WT is rated power.

	Life Time (y.r.)	Initial Cost ($)	Efficiency (%)	Power (kW)
INV	15	771.6	96	–
PV	24	1800	95	7.3
WT	24	2869	95	30

2.5. Energy storage systems

With the increasing demand for electrical energy to provide conditions for the use of appliances, smartphones, and even cars, new technologies for energy storage systems (ESS) have been proposed. In

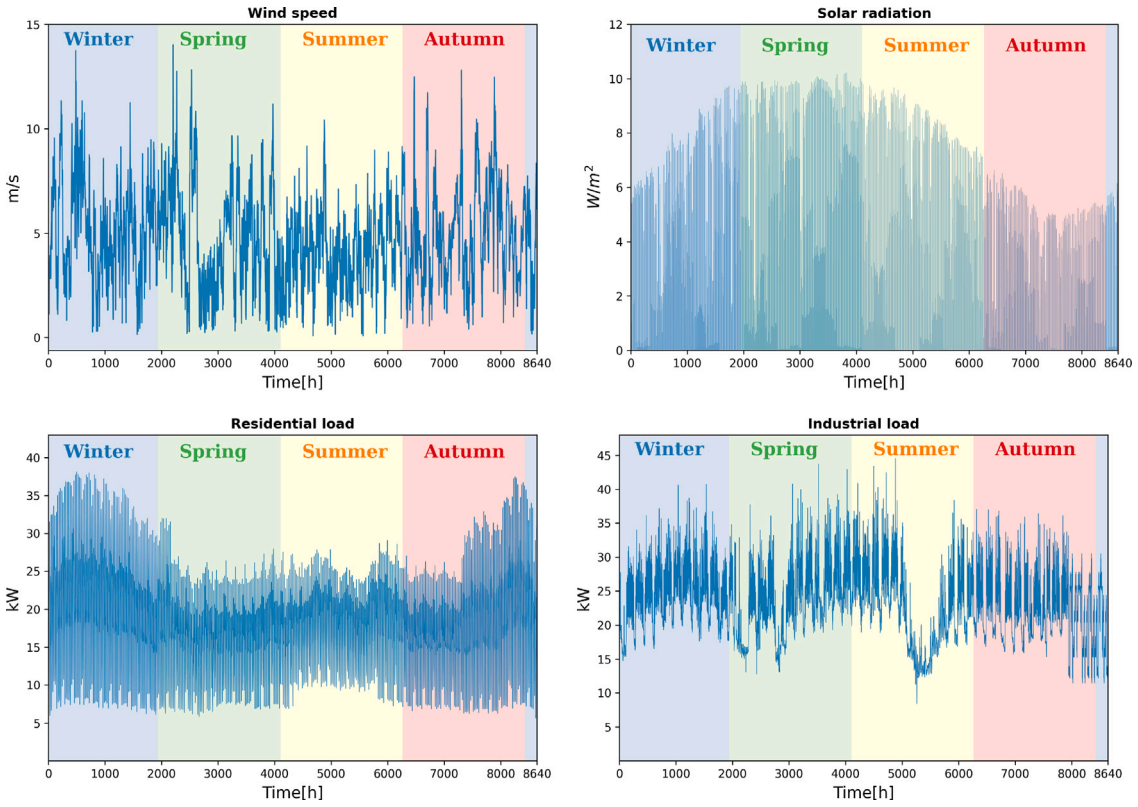

Fig. 2. Input system time series data: wind speed, solar radiation, and loads.

general, to design new storage systems some characteristics need to be taken into account: (i) the scalability/power bridging to provide and guarantee proper management in power generation for charge/discharge operation over the use of equipment (in the period of multiple hours); (ii) ESS needs to operate in a fast response time to supply fast discharge capabilities making the equipment more versatile; (iii) in general, a battery must have a high storage capacity that means the ability to store power energy for a long period of time; (iv) in ESS, the price is an important issue in which the costs of storage need to be competitive in the market, (taking into account the cost–benefit); (v) the efficiency of an ESS is correlated to its storage capacity and its ability to reduce energy losses in the charge/discharge operation (the better the ESS fulfills these requirements, the greater its efficiency); (vi) it is desirable for an ESS to have a long life. It means that, in a general way, the storage system should be a good trade-off between use life and maintenance activity of the equipment, and; (vii) finally, the battery needs to present a low environmental impact indicating that ideally, the storage maintains a low level of pollutant emissions in its operation throughout its use [84–87].

To study new technologies, this work aims to simulate an hybrid microgrid system (HMGS) in order to test different ESS. In particular, two promising ESS technologies are: a technology based on Vanadium redox flow batteries (VRFB – [46]) and one based on spinel lithium titanate ($Li4Ti5O_{12}$ (LTO) – [45]). In recent decades, interest in redox flow batteries has gained attention as the demand for energy storage has grown. This is due to the emerging market for electricity production via solar and wind power [87]. According to [88], VRFB is able to provide modular and scalable energy in terms of an easy scale-up, long cycle life, and good recyclability.

Table 2
ESS techno-economic values.

Factor	Unit	Generic	VRFB	LTO
Cycles	un	5000	10,000	8000
Cost	$/kWh	1256.00	581.66	1143.00
Efficiency	%	70	75	90
Lifetime	y.r.	20	15	17.5
BoP	$/kW	374	374	374
Other cost	$/kW	328	328	328

The main advantages of VRBF are twofold. It presents a fast response in its operation (loading and unloading taking less than 0.001 s). It also presents a high capacity for carrying out operating cycles (no less than 10,000 and up to more than 16,000 cycles). However, VRBF still has a high cost when compared to other technologies. Moreover, it is responsible for energy losses in the system [46,89].

LTO has been studied in the 1980s as a cathodic material for lithium-ion batteries because of its high conductive capacity. However, it has not attracted wide attention due to its low potential and low discharge capacity [90]. LTO is a technology with a high lithium insertion/extraction voltage of approximately 1.55 V (vs. Li/Li+) and excellent cycle stability. The significant advancement of LTO is the high efficiency (>90%), high energy density, rapid response time, and attractive self-discharge rate. It also shows a prolonged cycle operation (8000 full cycles) and 20 years of lifetime [91]. However, as a disadvantage LTO has a higher cost [44,92]. Table 2 shows a brief overview of the main techno-economic characteristics of the considered ESS in this work.

3. Proposed evolutionary swarm solution

Electrical power flow problems very often contain several local minima along with high dimensional search space and a mix of continuous and integer variables. These characteristics pose difficulties for many standard optimization techniques that are overcome in evolutionary meta-heuristics. Among the many available meta-heuristics, swarm intelligence algorithms are constantly being successfully applied in solving electrical energy flow problems [73,93–95]. A recent algorithm namely Canonical Differential Evolutionary Particle Swarm Optimization (C-DEEPSO) has been proposed in [69] and has been effectively solving problems related to optimal power flow in electrical systems. This algorithm is a swarm-based optimization technique that implements selection and mutation operators derived from Differential Evolution (DE), initially proposed by [96]. The recombination operator employed in C-DEEPSO is borrowed from the Particle Swarm Optimization (PSO) proposed by [97].

C-DEEPSO's movement rule equation is the same as presented by the main swarm intelligence algorithms, according to Eq. (15)

$$\mathbf{X}_n = \mathbf{X}_{n-1} + \mathbf{V}_n \tag{15}$$

Notwithstanding, not only the velocity in C-DEEPSO differs from the standard swarm intelligence techniques but also the way the best particles are stored. C-DEEPSO uses a memory mechanism that saves a percentage of the best particles found so far among the particles in the population. By using this mechanism, the new velocity is calculated by Eqs. (16) and (17),

$$\mathbf{V}_n = \mathbf{w}_I^* \mathbf{V}_{n-1} + \mathbf{w}_A^* (\mathbf{X}_{sn} - \mathbf{X}_{n-1}) + \mathbf{w}_C^* \mathbf{C} (\mathbf{X}_{gb}^* - \mathbf{X}_{n-1}), \tag{16}$$

$$\mathbf{X}_{sn} = X_{rand} + F(X_r - X_{n-1}). \tag{17}$$

The first term in this equation is the inertia term, related to the previous velocity. The second term is the assimilation term that uses an evolutionary strategy that comes from DE. In this work, the *rand/1/bin* strategy is used to generate, according to Eq. (17). The particle $\mathbf{X}_r$ is obtained from uniform recombination from the particles in the memory. Finally, the third term in Eq. (16) is the communication term, in which $\mathbf{X}_{gb}$ stands for the global best particle ever found and the term $\mathbf{C}$ represents a $N \times N$ diagonal matrix of random variables sampled in every iteration. These random variables are sampled according to a Bernoulli distribution with success probability P that provides the communication among the particles (see [98]). The superscript * indicates that the corresponding parameter undergoes evolution through a mutation process using a Gaussian distribution given by Eq. (18):

$$w^* = w[1 + \tau \times N(0,1)]. \tag{18}$$

We applied C-DEEPSO to solve the optimization problem composed by Eq. (12) added to the constraint of generating energy preferably from renewable sources. The optimization problem has four decision variables with the respective bounds: nominal power of the PV ([10,150] kW); autonomy grade for the BESS ([1,3] hours); the number of wind turbines ([1,5] units), and nominal power of the public grid ([1, 100] kW). The movement rule (see Eq. (16)) is applied to find the initial velocity for all particles in swarm, according to: $V0 = v_{min} + ((v_{max} - v_{min})) \times rand(1, D)$ in which, the minimal velocity is $v_{min} = UPPER_{bound} - LOWER_{boud}$, the maximal velocity for a particle is $v_{max} = \left|v_{min}\right|$, and D is the dimension of electric dispatch in HMGS problem. Fig. 3 presents a diagram of the solution applied to electric power generation in the HMGS grid-connected described by Algorithm 1.

Algorithm 1 C-DEEPSO for HMGS

Require: population size (NP), mutation rate τ, communication rate (P), memory size (MB), total iterations (T), lower bounds ($X_{lb}^{PV}, X_{lb}^{WT}, X_{lb}^{ESS}, X_{lb}^{PG}$) and upper bounds ($X_{ub}^{PV}, X_{ub}^{WT}, X_{ub}^{ESS}, X_{ub}^{PG}$), renewable factor constraint (rc), seasonal data series, components characteristics,
Set the generation number $t = 0$
Initialize the NP particles positions and velocities at random according to $[\mathcal{U}(X_{lb}^{PV}, X_{ub}^{PV}), \mathcal{U}(X_{lb}^{WT}, X_{ub}^{WT}), \mathcal{U}(X_{lb}^{ESS}, X_{ub}^{ESS}), \mathcal{U}(X_{lb}^{PG}, X_{ub}^{PG})]$
Evaluate the renewable factor of the initial population
while *renewable factor* $> rc$ **do**
  Initialize the NP particles positions and velocities at random according to $[\mathcal{U}(X_{lb}^{PV}, X_{ub}^{PV}), \mathcal{U}(X_{lb}^{WT}, X_{ub}^{WT}), \mathcal{U}(X_{lb}^{ESS}, X_{ub}^{ESS}), \mathcal{U}(X_{lb}^{PG}, X_{ub}^{PG})]$
  Evaluate the renewable factor of the initial population
end while
Update the global best X_{gb} with minimum COE and LOLP
while $t < T$ **do**
  for individual i in the population NP **do**
    Calculate X_r using the strategy $S_g P_B - rnd$
    Copy current individual X_{t-1}
    Mutate strategy parameters w_I, w_A, w_C and X_{gb}^*
    Apply movement rule in current individual according to Equations (15) and (16)
    X_{t-1}
    Evaluate current individual X_t and its copy
    Select the fittest individual to proceed to next generation
    Update personal best individual
    Update global best individual
  end for
  $t = t + 1$
end while

4. Experiments and results

In this section, we evaluate the impact of Net Metering when applied to MG. Furthermore, the evaluation of two distinct ESS systems is carried out. The experimental setup is divided into the following studies:

1. To assess the Net-Metering economical impacts on MG performance to solve the electric dispatch problem in HMGS, we perform 30 runs for each load profile scenario (residential and industrial). We use a generic ESS to measure the impact of Net metering in the grid using a compensation of 100%;
2. The VRFB and LTO are evaluated in the system using 25%, 50%, 75%, and 100% Net-Metering compensation. The obtained results are compared to the results of VRFB vs. LTO in each load scenario, and;
3. To analyze the optimized results for solving the electrical dispatch problem, highlighting the positive impact of using this approach as a power production control system capable of generating great savings for prosumers users.

For assessing the performance of the experiments, the initialization parameters used for C-DEEPSO are a population size equal to 10 particles, and the total number of iterations equal to 20 (stop criteria). The algorithm uses a mutation rate equal to 0.5 and a communication rate equal to 0.9. All parameters have been defined empirically. We conducted the computational simulation using an Intel(R) Core(TM) i9-10900X CPU@3.70 GHz and 64 GB RAM, with Windows 10 Pro. The simulation code is implemented in Matlab R2020b.

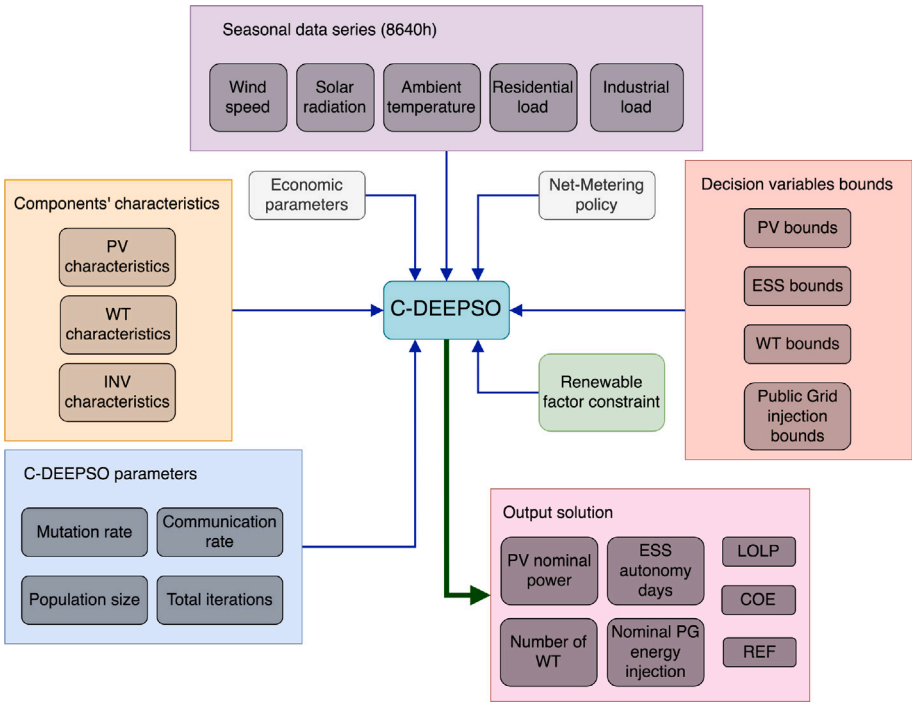

Fig. 3. Diagram describing C-DEEPSO applied to the HMGS modeled.

4.1. MG vs. MG with net-metering

In this experiment, we propose the analysis of the impact of the Net-Metering policy on the MG system modeled in this work. For this, 30 runs for each scenario, with and without Net-metering, were performed. A generic battery was considered in the MG and its information is shown in Table 2. We analyzed the average result, considering a 100% energy offset between the MG and the public grid. From the averages of the optimized solutions using the generic battery, an analysis of the behavior of the MG was performed. Industrial load refers to the monitoring of real industrial activity. The time series was normalized to meet a consumption of 6 000 000 kWh per year.

A generic battery is implemented as ESS with its state of charge (SoC) shown across scenarios. The maximum charge power depends on the SoC. When SoC is 100% (completely charged), the power is limited by the maximum capacity the battery converter can provide. Power charging is maintained almost constant until the ESS's SoC reaches around 80%. Then, the charging ESS is progressively reduced, to avoid too high battery voltages that could damage it. The generation of energy produced in the spring and winter periods for the industrial load can be analyzed in Figs. 4(a) to 4(d). The residential load for the same periods can be observed in Figs. 4(e) to 4(h). In all scenarios, it is possible to notice the charging and discharging of the ESS by the variation of the SoC. Fig. 5 depicts the ESS's SoC along with its charging and discharging amounts. It is important to note that the Net-Metering policy affects only the behavior of the controller when consuming from the public grid. Hence, Fig. 5 does not distinguish between the presence or absence of a Net-Metering policy.

Observing Figs. 4(a) and 4(e), we can see that even though both scenarios present peaks near 130 kW of power load during Spring. The electrical supply needed in the industrial scenario oscillates around 80 kW and in the residential scenario, it showed lower values close to 30 kW. As a result of the higher amplitude of the power demand curve in the residential scenario, the public grid consumption is lower than that in the industrial scenario. In addition to this, ESS in the industrial scenario takes more hours to fully charge, as shown by the differences in the charging behavior presented in Figs. 5(a) and 5(c). Moreover, the well-behaved load in the residential scenario allows the ESS's discharging peaks to align with the moments of higher load. The continuously high power necessity in the industrial scenario surpasses the amount of renewable energy available, which incurs falling back to the public grid multiple times in order to attend the system. Furthermore, we can see in Figs. 4(c) and 4(g) that, during Spring, all public network generation can be compensated via the Net-Metering policy in both industrial and residential scenarios.

Analyzing Figs. 4(b) and 4(f), it is possible to note that, while industrial power load does not vary too much between 30 kW and 80 kW in Winter, the residential scenario's amplitude is even higher than that in Spring, ranging from 30 kW to more than 130 kW. Moreover, when the amount of available energy from PV and Wind is low in Winter, the ESS is not able to fully handle these power request spikes in the residential scenario. In Fig. 5(d) we can see that the battery is not only discharged more rapidly but also is fully discharged before the hours with the highest load. This type of behavior leads to using the public grid multiple times, achieving peaks in public network energy of more than 180 kW. On the other hand, the behavior of load in the industrial scenario can be mostly satisfied by renewable energy sources with a minor call to the public network. This demand increases only when the incidence of wind and solar radiation reduces drastically. Unlike Spring, the low PV and Wind generation associated with a high energy requisition does not allow all the public grid to be compensated via the Net-Metering policy. In Fig. 4(d), we can see that the low variability in the industrial load allows almost all the public network generation to be compensated via Net-Metering. However, as shown in Fig. 4(h), the extremely high peaks of public network generation in the residential scenario cannot be fully compensated via Net-Metering. Additionally, Fig. 5(b) shows that when the energy request does not vary much as in the industrial scenario, the ESS is discharged slower when compared to the residential scenario. Thus, when renewable energy generation is low, as in Winter, the shape of the power load curve directly influences both the amount of public network generation that can be compensated via Net-Metering and the charging/discharging behavior of the ESS deployed in the MG.

To verify the impact of the net-metering policy on the system, Fig. 6 presents the result of the annual generation in the industrial scenario.

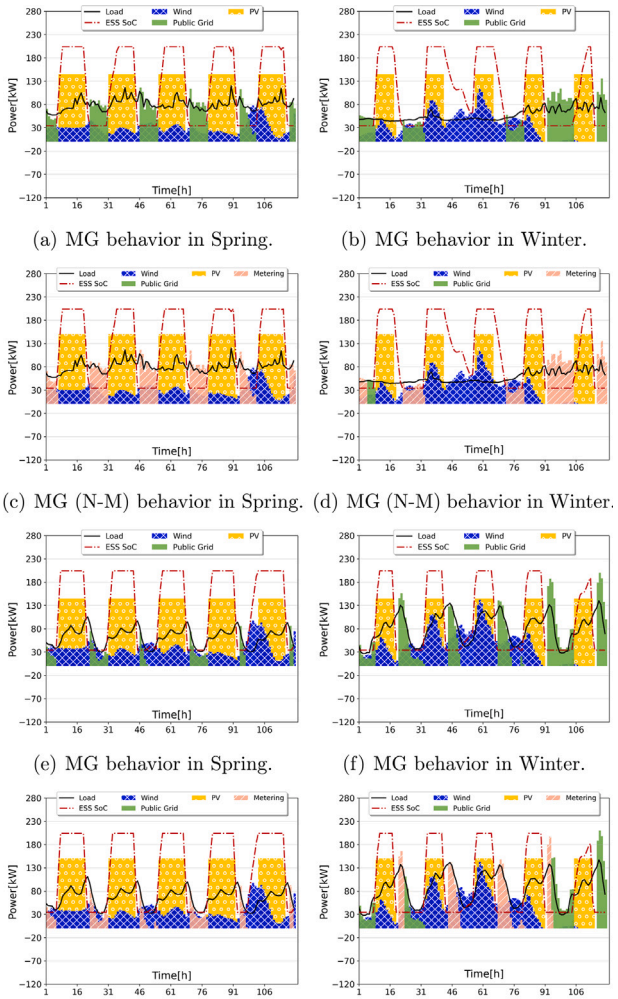

(a) MG behavior in Spring. (b) MG behavior in Winter.

(c) MG (N-M) behavior in Spring. (d) MG (N-M) behavior in Winter.

(e) MG behavior in Spring. (f) MG behavior in Winter.

(g) MG (N-M) behavior in Spring. (h) MG (N-M) behavior in Winter.

Fig. 4. Industrial (a–d) and Residential (e–h) analysis. N-M stands for Net-Metering.

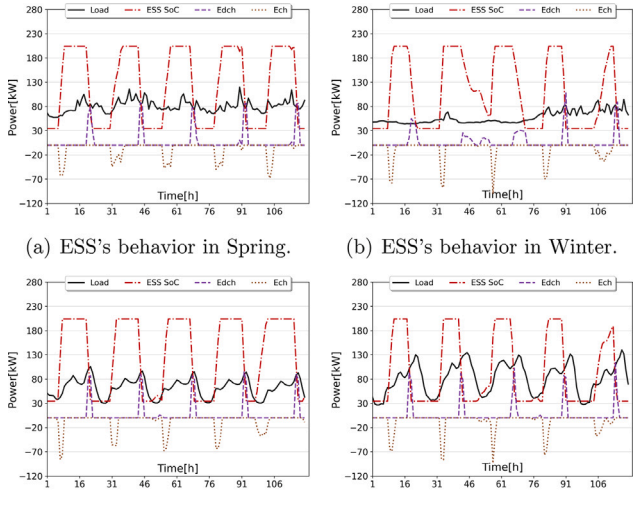

(a) ESS's behavior in Spring. (b) ESS's behavior in Winter.

(c) ESS's behavior in Spring. (d) ESS's behavior in Winter.

Fig. 5. Industrial (a–b) and Residential (c–d) ESS's behavior analysis.

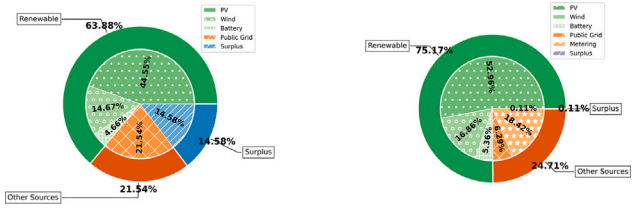

(a) MG without Net-Metering (b) MG with Net-Metering.

Fig. 6. Total annually generation share in industrial scenario.

The total power generation without a Net-metering policy is shown in Fig. 6(a). We can see that the renewable production, composed of solar, wind, and ESS was 63.88% in a year. When the MG was not able to generate energy from these sources, due to seasonal fluctuations of low solar radiation or low wind speed, the MG resorted to the public grid to meet the load. The surplus situation in which renewable sources are already supplying the demand and the ESS is fully charged, composed 14.58% of the total power generation that cannot be used locally. When applying the Net-metering policy, as shown in Fig. 6(b), the renewable factor was 75.17%. This means an increase of 11.29% of the generation provided by renewable generators. The compensation generated reduces the need to inject energy via the public grid and, in the industrial scenario, the Net-Metering policy has benefited the system to the point of reducing substantially the MG surplus (being just 0.11%).

Fig. 7 shows the total generation in the residential scenario. We can note that the Net-Metering policy adopted in Fig. 7(b) increased the usage of renewable energy sources, compared to Fig. 7(a). The MG without Net-Metering policy had as a renewable share of just 66.11% of power production. On the other hand, in the MG with Net-Metering policy, the renewable share was 76.51% of energy power. It means an increase of 10.4% in the share comprised of PV panels, wind generators, and ESS. In this case, the surplus was even smaller (0.03%) when compared to the surplus of the MG without the Net-Metering policy. The supplementation of energy via the public network was even lower when compared to the industrial scenario. Here, the difference was 12.02%. An interesting fact is the increase in ESS usage when the Net-metering policy is used.

In terms of power energy prices, the generation in the industrial scenario was 61.ct$ per kWh without the Net-metering policy. When we used 100% of compensation, the final price was 28.ct$ per kWh. This means an economy of 33.ct$ per kWh. Similar behavior is observed in the residential scenario. MG attending the residential load without the compensation policy had a cost of 55 ct per kWh, and using Net-Metering a cost of 28.ct$ per kWh, generating an economy of 27.ct$ per kWh. In general terms, it is noted that the use of a compensation policy benefits generation in MG systems. The energy surplus is almost zero, the use of the ESS system is more effective, and the generation cost reduction is, on average, 48% smaller in relation to the two load scenarios studied. The losses of power supply probability (LOLP) were less than 5% in all cases.

4.2. Discussion about ESS technologies: VRFB vs. LTO

Following the previous analysis of the MG behavior when an N-M policy is applied, we study the effects of different battery technologies in the MG. Therefore, two new emerging ESS technologies, the Vanadium redox flow batteries (VRFB) and the Spinel Lithium Titanate ($Li4Ti5O_{12}$) batteries (LTO), are evaluated in terms of loss of load probability, costs, penetration of renewable energy and excess power. As discussed in Section 2.5, these technologies differ in terms of efficiency, cost, and the number of cycles, among other particulars. LTO is 20% more efficient than VRFB. On the other hand, VRFB has 2000 more

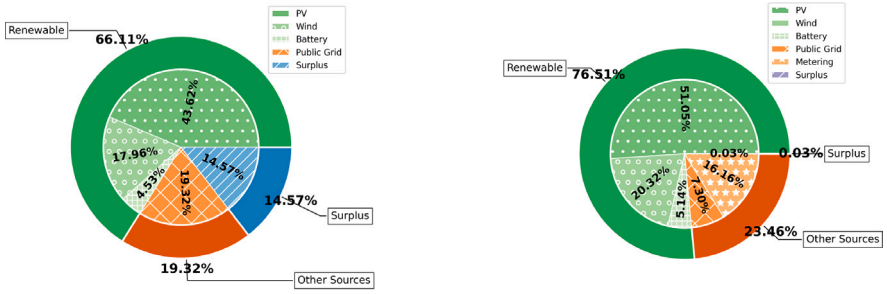

(a) MG without Net-Metering (b) MG with Net-Metering.

Fig. 7. Total annually generation share in residential scenario.

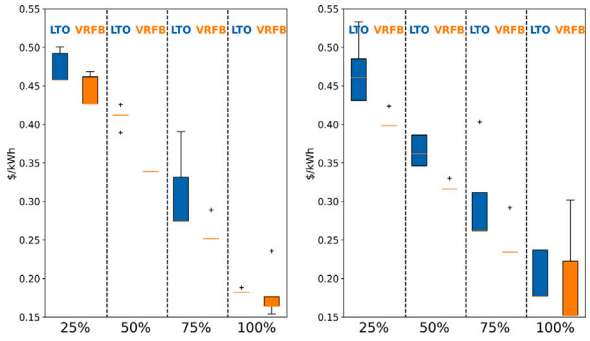

(a) Costs in Industrial case (b) Costs in Residential case.

Fig. 8. Boxplot of industrial and residential optimized prices in MG.

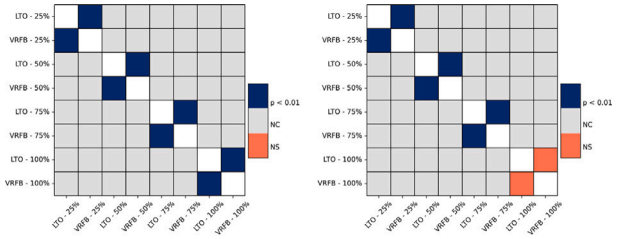

(a) Industrial case (b) Residential case.

Fig. 9. Heatmap of the pairwise comparisons after applying the Conover test with Holm–Bonferroni correction using 99% of confidence level. Legend: $p < 0.01$ indicates that the test is significant; NS indicates that the test is not significant; NC indicates pairwise comparisons with different compensation percentages that are not considered.

track cycles than LTO. We followed the same experimentation procedure discussed in Section 4.1. All tests followed the same generation behavior, indicating that both batteries charge and discharge energy. Table 3 shows the average results obtained by the ESSs studied here, when used in the MG for the industrial and residential test scenarios after 30 runs.

When the microgrid employs a Net-Metering policy, both the industrial and residential scenarios can experience a reduction in the LOLP. Analyzing Table 3, we can see that, in the industrial scenario, there is a reduction of 0.18% using LTO battery with 100% compensation and 0.19% using VRFB battery with 25% compensation. In the residential scenario, the reduction in the LOLP is 0.44% using LTO battery with 50% compensation and 0.30% using a VRFB battery with 100% compensation. It is possible to see in Table 3 that the more energy compensation is performed in the MG (in terms of %), the lower the final value of kWh (in $). In all cases the use of renewable sources increases, reaching a value greater than 76% in some cases. Furthermore,

Table 3
ESS mean results according Net-Metering level's (0%: without compensation).

	LOLP	COE	REF	Surplus
Industrial				
LTO (0%)	5.34%	50.ct$	69.98%	20%
VRFB (0%)	5.31%	47.ct$	69.83%	19%
LTO (25%)	5.24%	47.ct$	74.64%	<1%
VRFB (25%)	5.12%	44.ct$	74.16%	<1%
LTO (50%)	5.32%	41.ct$	73.66%	<1%
VRFB (50%)	5.16%	34.ct$	75.22%	<1%
LTO (75%)	5.21%	30.ct$	74.64%	<1%
VRFB (75%)	5.17%	26.ct$	75.05%	<1%
LTO (100%)	5.16%	18.ct$	75.64%	<1%
VRFB (100%)	5.23%	18.ct$	75.20%	<1%
Residential				
LTO (0%)	5.82%	49.ct$	70.74%	18%
VRFB (0%)	5.50%	44.ct$	72.08%	19%
LTO (25%)	5.50%	47.ct$	74.57%	<1%
VRFB (25%)	5.22%	40.ct$	76.46%	<1%
LTO (50%)	5.38%	37.ct$	76.23%	<1%
VRFB (50%)	5.25%	32.ct$	76.69%	<1%
LTO (75%)	5.42%	30.ct$	75.64%	<1%
VRFB (75%)	5.32%	25.ct$	76.37%	<1%
LTO (100%)	5.39%	20.ct$	76.41%	<1%
VRFB (100%)	5.20%	20.ct$	75.67%	<1%

disregarding Net-Metering, the MG shows a surplus higher than 18% in all cases.

We can note the impact of the distinct ESS technologies, LTO and VRFB, in the power generation in terms of objective functions used in this work. VRFB showed fewer prices in all cases (applying or not the Net-Metering policy). In addition, in only one case, the LTO presented a renewable factor greater than the VRFB (in both cases with 100% compensation). Evaluating the losses generated in the system (LOLP) and the occurrence of surplus, we see that both batteries had similar results in all cases. On average, the kWh in Spain is 0.4892 $/kWh. Thus, when using the VRFB or LTO in the microgrid with compensation policies, the generation costs were lower than the average price of $/kWh in Spain. Table 3 shows a summary of tests performed.

This fact validates the power micro-generation of energy as a good way to achieve the energy goals in Spain. Fig. 8 presents boxplots of KWh price values (in $) in the MG, using LTO and VRFB, for different compensation policies. Each boxplot displays the summary of the price values (minimum, first quartile, median, third quartile, and maximum) obtained for each battery technology using 25%, 50%, 75%, and 100% compensation values. In this kind of analysis, when the boxes do not overlap, we can say that there is a statistical difference between the sample mean represented by the non-overlapped boxes [98]. However, when the boxes overlap, further investigation is required to assess if there is a statistical difference between the obtained sample means.

Observing Fig. 8(a), for the industrial case, the VRFB proves to be a more promising technology than LTO showing an average lower price

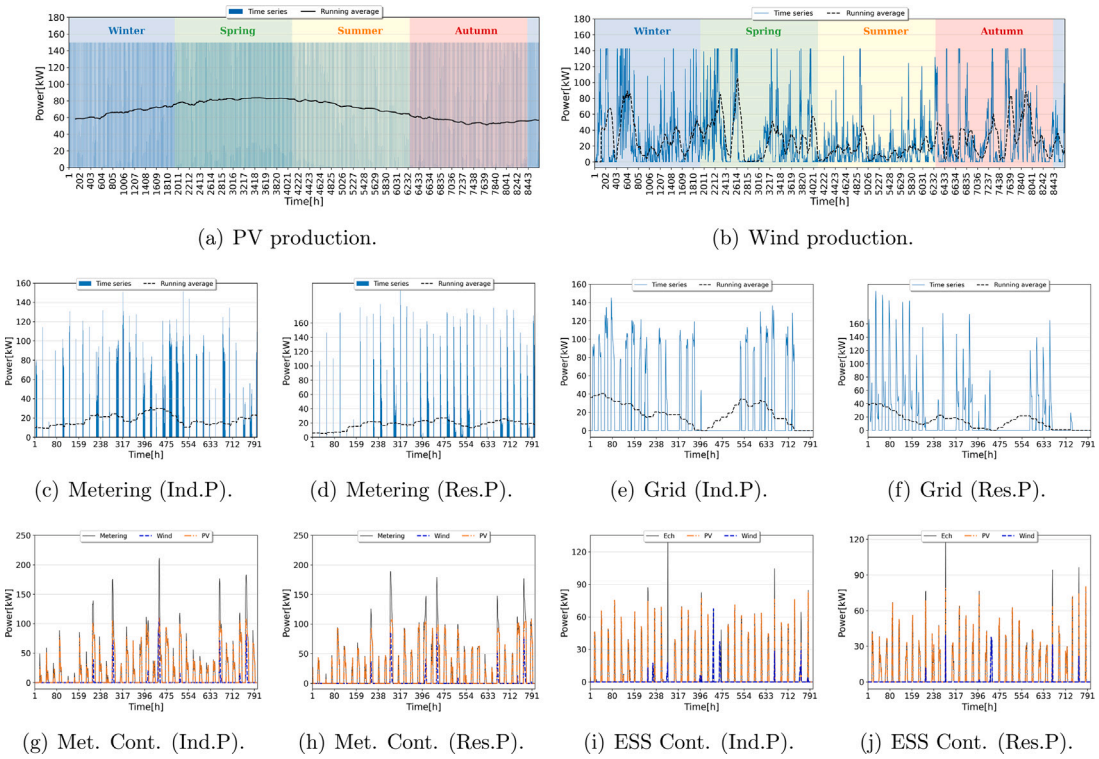

(a) PV production. (b) Wind production.

(c) Metering (Ind.P). (d) Metering (Res.P). (e) Grid (Ind.P). (f) Grid (Res.P).

(g) Met. Cont. (Ind.P). (h) Met. Cont. (Res.P). (i) ESS Cont. (Ind.P). (j) ESS Cont. (Res.P).

Fig. 10. Electrical results. Production to Industrial (Ind.P) | Production to Residential (Res.P). Contribution (Cont.).

result for all compensation policies. Except for the 25% case, all the boxes do not overlap, indicating that VRFB mean-cost of energy result is statistically different from LTO battery. Considering the residential case, a similar conclusion can be derived for all compensation policies excluding 100%. In this work, we defined the null hypothesis as the equality of the mean costs obtained after 30 runs for each scenario. After that, we applied a statistical test to ensure in which pairs of comparisons the null hypothesis can be rejected or not, for a given significance level α. To assess the test results, we analyze the p-values obtained. A p-value is the likelihood that, in a sample, the null hypothesis is correct [99]. For a significance level of $\alpha = 0.01$, when the p-value ≤ 0.01, we can say that there are no differences among the mean values being compared with a 99% confidence interval [98]. Thus, we chose a nonparametric test entitled Conover statistical test [100] along with Holm–Bonferroni correction[1] [101] to evaluate the samples of energy costs obtained from the system using either LTO or VRFB technologies in the smart grid, applied to both test scenarios (residential and industrial). Fig. 9 shows the Conover test results as a heatmap, in which the diagonals immediately above and below the main one provide the test outcomes for each pairwise comparison. A blue square indicates that it was possible to find differences between the compared mean costs, rejecting the null hypothesis, because the p-value obtained is less than 0.01. Fig. 9(a) shows that, for the industrial case test results, all pairs are significant. Thus, we can say that, with 99% confidence, VRFB is the alternative with the lower cost for all the compensation levels evaluated in the industrial scenario. Additionally, the same can be stated for the VRFB in the residential scenario in Fig. 9(b) with 25%, 50%, and 75% compensation levels. The test nonetheless was not able to identify differences between the LTO and VRFB mean costs for the 100% compensation level in the residential scenario.

To summarize, Table 4 shows an overview of the costs obtained for each battery technology under the evaluated Net-Metering levels. As a validation of the minimum average cost obtained, the plus sign (+) besides VRFB indicates that the mean cost for this battery is significantly different (with 99% confidence) from the cost for a LTO battery with a minus sign (−). We can observe that, apart from the results obtained for a 100% compensation level, VRFB obtained both statistically significant costs and a smaller standard deviation. This result indicates that the VRFB technology consistently achieved lower kWh costs through runs.

In general, we can say VRFB proves to be a suitable option since both the mean and standard deviation cost values found by the compensation policies are lower than that of LTO. One can argue that either for the residential or industrial cases when the compensation is set to 100%, it may be economically advantageous for the prosumer to choose LTO. Although the difference in the prices is not statistically significant in the residential scenario, its useful life is longer than that of VRFB and it provides a smaller cost variation.

4.3. Discussion about the optimal controller and the savings achieved

Since in Spain the Net-metering policy has not been implemented yet, we only analyzed the use of this compensation policy for the 25% level, in a conservative way, to show the benefits of applying Net-Metering. For a better discussion about the functioning MG generation, an evaluation of the characteristics of power generation in the MG is described with the VRFB storage system. Furthermore, we chose a time interval in the winter season to analyze the general behavior of the microgrid system.

Fig. 10 represents a compilation of generation results in kW. The energy production by PV sources and wind generators is the same for both scenarios (residential and industrial), as the time series of wind and solar radiation are the same. Fig. 10(a) shows a trend curve obtained by calculating the moving average for a week that helps a visual analysis. As expected, there is a greater production of solar energy in the mid-spring and mid-summer periods, with an average of 80 kW. A

[1] The correction is used along with the test to alleviate the influence of multiple comparisons in the final test results by controlling the family-wise error rate.

Table 4
Summary of the obtained costs on each scenario. A plus sign (+) indicates that, within the same Net-Metering level, the battery cost is significantly different from the other with the minus sign (−).

N-M Level	Battery	Best	Median	Worst	Mean	Std.
Industrial						
25%	(−)LTO	46.ct$	46.ct$	50.ct$	47.ct$	1.9.ct$
	(+)VRFB	43.ct$	43.ct$	47.ct$	44.ct$	1.9.ct$
50%	(−)LTO	39.ct$	41.ct$	43.ct$	41.ct$	1.2.ct$
	(+)VRFB	34.ct$	34.ct$	34.ct$	34.ct$	0.0.ct$
75%	(−)LTO	27.ct$	27.ct$	39.ct$	30.ct$	4.5.ct$
	(+)VRFB	25.ct$	25.ct$	29.ct$	26.ct$	1.5.ct$
100%	(−)LTO	18.ct$	18.ct$	19.ct$	18.ct$	0.2.ct$
	(+)VRFB	15.ct$	16.ct$	24.ct$	18.ct$	2.9.ct$
Residential						
25%	(−)LTO	43.ct$	46.ct$	53.ct$	47.ct$	3.9.ct$
	(+)VRFB	40.ct$	40.ct$	42.ct$	40.ct$	1.0.ct$
50%	(−)LTO	35.ct$	36.ct$	39.ct$	37.ct$	1.8.ct$
	(+)VRFB	32.ct$	32.ct$	33.ct$	32.ct$	0.6.ct$
75%	(−)LTO	26.ct$	26.ct$	40.ct$	30.ct$	5.6.ct$
	(+)VRFB	23.ct$	23.ct$	29.ct$	25.ct$	2.3.ct$
100%	(−)LTO	18.ct$	18.ct$	24.ct$	20.ct$	2.9.ct$
	(−)VRFB	15.ct$	15.ct$	30.ct$	20.ct$	6.0.ct$

higher autumn/winter wind power generation rate (maximum installed turbine capacity of 240 kW) is seen in Fig. 10(b). The dispersion of wind generation is greater due to the air currents that may have occurred during the year in the studied region.

It is noted that energy compensation in winter is more effective in the industrial setting when comparing Figs. 10(e) and 10(c). The Net-Metering in industrial load is on average 20 kW higher than in the residential load between hours 317 and 554. The contribution of solar and wind sources to generate the Net-Metering can be seen in Figs. 10(g) and 10(i). Results indicate that power generation via PV panels has a greater contribution when compared to generation via wind turbines. The Net-Metering for the period presents peaks of high power generated, sometimes reaching more than 150kw in both loads tested.

Electricity from the public grid is only used in the MG model when demand cannot be met by renewable sources, battery storage, and in the absence of a positive energy balance to be compensated, as illustrated in Figs. 10(e) and 10(f). The average fluctuation of the amount of electricity consumed from the public grid is more intense in the industrial scenario, with peaks of 40 kW. Contrarily, the residential load scenario, for the same period, presents a low need to resort to the public grid to maintain the necessary load that serves the 200 houses. Although there is a high ESS charge contribution from wind generation on some days in the industrial scenario, we can say, by analyzing Figs. 10(i) and 10(j), that most part of the energy used to charge the ESS comes from the solar source, for both load profiles.

Fig. 11 shows both the MG and the ESS behavior in relation to available energy sources using VRFB with 25% of Net-Metering for industrial/residential electrical supply during the winter. As illustrated by Figs. 11(a) and 11(b), the PV generation is by far the source that most contributes to the MG system, reaching more than 50% of generation for both load scenarios. Figs. 11(c) and 11(d) show that VRFB works by keeping the SoC stable and presenting charge (Ech) and discharge (Edch) states properly. In particular, this ESS is well suited to provide modular and scalable energy storage due to favorable characteristics that validate its use.

By analysing the residential scenario in Fig. 12(b), it is possible to notice that the maximum charge amount verified in the ESS was approximately 130 kW in some hours (in relation to PV/Wind), while the discharge was around 140 kW with peaks over 150 kW in winter. We argue that the operation for the residential VRFB loading and unloading profile is more efficient according to the technical specifications [51], This means that the microgrid benefits more from using the energy storage system because VRFB can provide high DoD without incurring in an increase in the life cycle loss [51]. This corroborates the use of this ESS by residences due to its quality and lower cost compared to LTO.

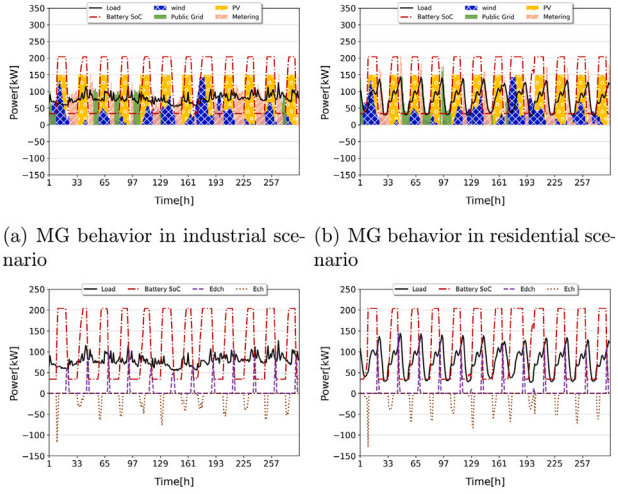

(a) MG behavior in industrial scenario (b) MG behavior in residential scenario

(c) ESS behavior in industrial scenario. (d) ESS behavior in residential scenario.

Fig. 11. MG meeting the industrial load demand (left) and residential load demand (right).

For the industrial load scenario, VRFB also shows its efficiency in terms of charge and discharge, bringing benefits to the MG. It is possible to verify that the maximum load verified in the system ESS was around 100 kW (relative to PV/Wind), while the discharge was around 100 kW (in relation to the load). From these results, it is possible to say that with a Net-Metering policy of 25% compensation, the VRFB battery efficiently meets the microgrid for both analyzed load profiles. The level of compensation between the MG and the public grid reduced the energy surplus to a value of less than 1%.

Comparing the values in Table 3, there is reduction in the industrial profile from 47ct.$ to 44ct.$ while in the residential profile from 44ct.$ to 40ct.$. From this, the application of the adopted Net-Metering policy generates an annual saving (yr) of 44112.17$/yr and 31793.05$/yr in the residential and industrial load scenarios, respectively. Furthermore, without using the compensation policy (25%),

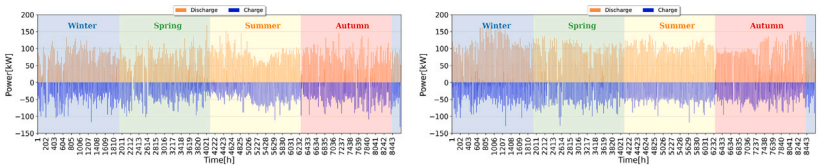

(a) VRFB operation in industrial scenario. (b) VRFB operation in residential scenario.

Fig. 12. Operation of the Vandium Redox Flow battery for Industrial and Residential loads.

the power surplus incurred in a waste of 90114.01$/yr (residential profile) and 82664.61$/yr (industrial profile). Thus, by employing a Net-Metering mechanism, the total amount saved is 134226.18$/yr and 114457.66$/yr for the residential and industrial load scenarios, respectively.

From this, the application of the adopted Net-Metering policy generates a reduction of thousands of dollars per year. This measure may have a positive impact on the economy, increasing the power to buy and sell energy in the national market, generating income for the prosumer. In addition, the study showed that ESS based on redox flow is beneficial to the microgrid, reducing the costs of kWh. Thus, the VRFB proved to be an interesting alternative when compared to a lithium-based battery.

5. Conclusions

In this paper, we have proposed new modeling for electric dispatch in microgrids (MGs) which takes into account the use of a Net-Metering (N-M) policy with different levels of compensation. The evaluated MG was composed of generic small wind turbines, photovoltaic panels, and an energy storage system (ESS). The proposed model is then optimized using an emerging evolutionary swarm meta-heuristic, the C-DEEPSO algorithm. Accordingly, we conducted a twofold analysis of industrial and residential scenarios, divided into three parts. First, the MG profile regarding energy sources contributions and surplus was analyzed before and after the inclusion of the Net-Metering policies. The evaluated Net-Metering policies differed according to the level of compensation, 25%, 50%, 75%, and 100%. Second, the ESS effects in the MG were analyzed according to lithium-based and redox flow-based battery specifications. Finally, the techno-economic impacts of employing a Net-Metering policy with a 25% compensation level are assessed and investigated.

In the first part of the analysis, the application of a 100% Net-Metering policy along with a generic ESS was evaluated. Results showed that the policy employed was beneficial to the system, reducing the excess energy (surplus) from 14.58% to 0.11% and from 14.57% to 0.03% in industrial and residential scenarios, respectively. Then, LTO and RFVB ESS technologies were evaluated without Net-Metering and with four different levels of Net-Metering: 25%, 50%, 75%, and 100%. The MG with N-M experienced in both consumption profiles a decrease in electrical power losses and an increase in the usage of renewable sources. In terms of energy costs, VRFB costs were statistically significant compared to LTO costs in both scenarios for compensation levels ranging from 25% to 75%. A MG with a 100% compensation level, however, will be better served by the LTO due to its longer life and smaller cost variation, even though both batteries have the same average kWh cost. In general, VRFB proved to be more efficient, even in the residential scenario in which the ESS is more intensely requested. Thus, an economical study was carried out in a MG using VRFB. This study showed that, in a conservative analysis, using a VRFB with a 25% N-M policy can yield prosumer savings larger than $134000.00 and $114000.00 per year for the industrial and residential profiles, respectively.

Regarding the evolutionary algorithm proposed, C-DEEPSO suffered from some drawbacks such that, mutation and communication parameters have to be carefully selected and, due to its stochasticity, several runs should be performed in order to assess an average result. Despite these drawbacks, an evolutionary swarm meta-heuristic like C-DEEPSO proved to be an efficient controller for electric dispatch in MGs. In summary, from a perspective of sustainability and energy savings, the results presented in this work gain relevance every day, representing tangible benefits for prosumers and for the environment in a future in which these types of systems are available to a larger portion of the population. As a future outcome, a sensitivity analysis can be performed evaluating not only ESS's cycle and calendar life but also its environmental impacts in a multi-objective approach.

CRediT authorship contribution statement

C.G. Marcelino: Conceptualization, Methodology, Software, Validation, Formal analysis, Investigation, Resources, Writing – original draft, Visualization, Writing – review & editing. **G.M.C. Leite:** Software, Validation, Formal analysis, Data curation, Writing – original draft. **E.F. Wanner:** Conceptualization, Methodology, Visualization, Investigation, Writing – original draft, Writing – review & editing. **S. Jiménez-Fernández:** Conceptualization, Methodology, Investigation, Supervision, Writing – review & editing, Project administration, Funding acquisition. **S. Salcedo-Sanz:** Conceptualization, Methodology, Investigation, Supervision, Writing – review & editing, Project administration, Funding acquisition.

Declaration of competing interest

The authors declare that they have no known competing financial interests or personal relationships that could have appeared to influence the work reported in this paper.

Data availability

No data was used for the research described in the article.

Acknowledgments

This project has received funding from the European Union's Horizon 2020 research and innovation programme under the Marie Skłodowska-Curie grant agreement No 754382. This research has been partially supported by Ministerio de Economía *y* Competitividad of Spain (Grant Ref. TIN2017-85887-C2-2-P) and by Comunidad de Madrid, PROMINT-CM project (grant No. P2018/EMT-4366). The authors thank UAH, UFRJ and CEFET-MG for the infrastructure used to conduct this work, and Brazilian research agencies: CAPES (Finance Code 001) and CNPq for support. "The content of this publication does not reflect the official opinion of the European Union. Responsibility for the information and views expressed herein lies entirely with the author(s)".

References

[1] Moorkens I, Tomescu M, Das A, Emele L. Renewable energy in Europe-2018: Recent growth and knock-on effects. TIK-Rep Eureopean Environ Agency 2018.

[2] Amoura Y, Ferreira ÂP, Lima J, Pereira AI. Optimal sizing of a hybrid energy system based on renewable energy using evolutionary optimization algorithms. In: Optimization, learning algorithms and applications. Cham: Springer International Publishing; 2021, p. 153–68.

[3] Zhang L, Yang Y, Li Q, Gao W, Qian F, Song L. Economic optimization of microgrids based on peak shaving and CO2 reduction effect: A case study in Japan. J Clean Prod 2021;321:128973. http://dx.doi.org/10.1016/j.jclepro.2021.128973.

[4] Li Y, Li K, Yang Z, Yu Y, Xu R, Yang M. Stochastic optimal scheduling of demand response-enabled microgrids with renewable generations: An analytical-heuristic approach. J Clean Prod 2022;330:129840. http://dx.doi.org/10.1016/j.jclepro.2021.129840.

[5] Luo X, Shi W, Jiang Y, Liu Y, Xia J. Distributed peer-to-peer energy trading based on game theory in a community microgrid considering ownership complexity of distributed energy resources. J Clean Prod 2022;351:131573. http://dx.doi.org/10.1016/j.jclepro.2022.131573.

[6] Tomin N, Shakirov V, Kozlov A, Sidorov D, Kurbatsky V, Rehtanz C, et al. Design and optimal energy management of community microgrids with flexible renewable energy sources. Renew Energy 2022;183:903–21. http://dx.doi.org/10.1016/j.renene.2021.11.024.

[7] Roslan M, Hannan M, Ker P, Mannan M, Muttaqi K, Mahlia T. Microgrid control methods toward achieving sustainable energy management: A bibliometric analysis for future directions. J Clean Prod 2022;348:131340. http://dx.doi.org/10.1016/j.jclepro.2022.131340.

[8] Marcelino C, Pedreira C, Baumann M, Weil M, Almeida P, Wanner E. A viability study of renewables and energy storage systems using multicriteria decision making and an evolutionary approach. In: Evolutionary multi-criterion optimization. Cham: Springer International Publishing; 2019, p. 655–68.

[9] Tarife R, Nakanishi Y, Chen Y, Zhou Y, Estoperez N, Tahud A. Optimization of hybrid renewable energy microgrid for rural agricultural area in Southern Philippines. Energies 2022;15(6). http://dx.doi.org/10.3390/en15062251.

[10] Mansouri S, Ahmarinejad A, Nematbakhsh E, Javadi M, Nezhad A, Catalao J. A sustainable framework for multi-microgrids energy management in automated distribution network by considering smart homes and high penetration of renewable energy resources. Energy 2022;245:123228. http://dx.doi.org/10.1016/j.energy.2022.123228.

[11] Kanakadhurga D, Prabaharan N. Demand side management in microgrid: A critical review of key issues and recent trends. Renew Sustain Energy Rev 2022;156:111915. http://dx.doi.org/10.1016/j.rser.2021.111915.

[12] Zhong X, Zhong W, Liu Y, Yang C, Xie S. Optimal energy management for multi-energy multi-microgrid networks considering carbon emission limitations. Energy 2022;246:123428. http://dx.doi.org/10.1016/j.energy.2022.123428.

[13] Shen Y, Hu W, Liu M, Yang F, Kong X. Energy storage optimization method for microgrid considering multi-energy coupling demand response. J Energy Storage 2022;45:103521. http://dx.doi.org/10.1016/j.est.2021.103521.

[14] Abou E-E, Adel A, El-Sehiemy R, Allam S, Shaheen A, Nagem N, et al. Renewable energy micro-grid interfacing: Economic and environmental issues. Electronics 2022;11(5). http://dx.doi.org/10.3390/electronics11050815.

[15] Manzano J, Salvador J, Romaine J, Alvarado L. Economic predictive control for isolated microgrids based on real world demand/renewable energy data and forecast errors. Renew Energy 2022. http://dx.doi.org/10.1016/j.renene.2022.05.103.

[16] Sajjad IA, Manganelli M, Martirano L, Napoli R, Chicco G, Parise G. Net-metering benefits for residential customers: The economic advantages of a proposed user-centric model in Italy. IEEE Ind Appl Mag 2018;24:39–49. http://dx.doi.org/10.1109/MIAS.2017.2740459.

[17] Badr M, Ibrahem M, Mahmoud M, Fouda M, Alsolami F, Alasmary W. Detection of false-reading attacks in smart grid net-metering system. IEEE Internet Things J 2022;9(2):1386–401. http://dx.doi.org/10.1109/JIOT.2021.3087580.

[18] Mehmood F, Umar M, Dominguez C, Kazmi H. The role of residential distributed energy resources in Pakistan's energy transition. Energy Policy 2022;167:113054. http://dx.doi.org/10.1016/j.enpol.2022.113054.

[19] Ansarin M, Ghiassi-Farrokhfal Y, Ketter W, Collins J. Economic inefficiencies of pricing distributed generation under novel tariff designs. Appl Energy 2022;313:118839. http://dx.doi.org/10.1016/j.apenergy.2022.118839.

[20] ANEEL. Resolução Normativa No. 482. 2015.

[21] Thakur J, Chakraborty B. Impact of increased solar penetration on bill savings of net metered residential consumers in India. Energy 2018;162:776–86. http://dx.doi.org/10.1016/j.energy.2018.08.025.

[22] Iglesias C, Vilaça P. On the regulation of solar distributed generation in Brazil: A look at both sides. Energy Policy 2022;167:113091. http://dx.doi.org/10.1016/j.enpol.2022.113091.

[23] do Brasil G. Lei 14.300. 2022.

[24] Kumar P, Malik N, Garg A. Comparative analysis of solar - battery storage sizing in net metering and zero export systems. Energy Sustain Dev 2022;69:41–50. http://dx.doi.org/10.1016/j.esd.2022.05.008.

[25] Jia X, Du H, Zou H, He G. Assessing the effectiveness of China's net-metering subsidies for household distributed photovoltaic systems. J Clean Prod 2020;262:121161. http://dx.doi.org/10.1016/j.jclepro.2020.121161.

[26] Londo M, Matton R, Usmani O, van Klaveren M, Tigchelaar C, Brunsting S. Alternatives for current net metering policy for solar PV in the netherlands: A comparison of impacts on business case and purchasing behaviour of private homeowners, and on governmental costs. Renew Energy 2020;147:903–15. http://dx.doi.org/10.1016/j.renene.2019.09.062.

[27] Wright S, Frost M, Wong A, Parton K. Australian renewable-energy microgrids: A humble past, a turbulent present, a propitious future. Sustainability 2022;14(5). http://dx.doi.org/10.3390/su14052585.

[28] Chakraborty P, Baeyens E, Khargonekar PP, Poolla K, Varaiya P. Analysis of solar energy aggregation under various billing mechanisms. IEEE Trans Smart Grid 2019;10:4175–87. http://dx.doi.org/10.1109/TSG.2018.2851512.

[29] Merodio M. The history in Spain of self-consumption with compensated excedents. 2022, https://www.magnuscmd.com/the-history-in-spain-of-self-consumption-with-compensated-excedents/.

[30] Rosales A, F. G, Diez D, Santos A. Photovoltaic self-consumption and net-metering: Measures to remove economic non-market failure and institutional barriers that restrict their use in Spain. In: Sea Water Desalination in Microgrids. Springer; 2022, p. 63–83.

[31] Hannan M, Faisal M, Jern-Ker P, Begum R, Dong Z, Zhang C. Review of optimal methods and algorithms for sizing energy storage systems to achieve decarbonization in microgrid applications. Renew Sustain Energy Rev 2020;131:110022. http://dx.doi.org/10.1016/j.rser.2020.110022.

[32] Fatin Ishraque M, Shezan S, Ali M, Rashid M. Optimization of load dispatch strategies for an islanded microgrid connected with renewable energy sources. Appl Energy 2021;292:116879. http://dx.doi.org/10.1016/j.apenergy.2021.116879.

[33] Li R, Zhang J, Zhao X. Dynamic wind farm wake modeling based on a bilateral convolutional neural network and high-fidelity LES data. Energy 2022;258:124845. http://dx.doi.org/10.1016/j.energy.2022.124845.

[34] Faraggiana E, Sirigu M, Ghigo A, Bracco G, Mattiazzo G. An efficient optimisation tool for floating offshore wind support structures. Energy Rep 2022;8:9104–18. http://dx.doi.org/10.1016/j.egyr.2022.07.036.

[35] Babaiahgari B, Ullah M, Park J-D. Coordinated control and dynamic optimization in DC microgrid systems. Int J Electr Power Energy Syst 2019;113:832–41. http://dx.doi.org/10.1016/j.ijepes.2019.05.076.

[36] Mosa M, Ali A. Energy management system of low voltage dc microgrid using mixed-integer nonlinear programing and a global optimization technique. Electr Power Syst Res 2021;192:106971. http://dx.doi.org/10.1016/j.epsr.2020.106971.

[37] Xin-Gang Z, Ze-qi Z, Yi-min X, Jin M. Economic-environmental dispatch of microgrid based on improved quantum particle swarm optimization. Energy 2020;195:117014. http://dx.doi.org/10.1016/j.energy.2020.117014.

[38] Siqin Z, Niu D, Wang X, Zhen H, Li M, Wang J. A two-stage distributionally robust optimization model for P2G-CCHP microgrid considering uncertainty and carbon emission. Energy 2022;124796. http://dx.doi.org/10.1016/j.energy.2022.124796.

[39] Bukar A, Tan C, Lau K. Optimal sizing of an autonomous photovoltaic/wind/battery/diesel generator microgrid using grasshopper optimization algorithm. Sol Energy 2019;188:685–96. http://dx.doi.org/10.1016/j.solener.2019.06.050.

[40] Bukar A, Tan C, Yiew L, Ayop R, Tan W-S. A rule-based energy management scheme for long-term optimal capacity planning of grid-independent microgrid optimized by multi-objective grasshopper optimization algorithm. Energy Convers Manage 2020;221:113161. http://dx.doi.org/10.1016/j.enconman.2020.113161.

[41] Baumann M, Domnik T, Haase M, Wulf C, Emmerich P, Rosch C, et al. Comparative patent analysis for the identification of global research trends for the case of battery storage, hydrogen and bioenergy. Technol Forecast Soc Change 2021;165:120505. http://dx.doi.org/10.1016/j.techfore.2020.120505.

[42] Andiappan V. Optimization of smart energy systems based on response time and energy storage losses. Energy 2022;258:124811. http://dx.doi.org/10.1016/j.energy.2022.124811.

[43] Li X, Palazzolo A. A review of flywheel energy storage systems: state of the art and opportunities. J Energy Storage 2022;46:103576. http://dx.doi.org/10.1016/j.est.2021.103576.

[44] Zou T, Luo L, Liao Y, Wang P, Zhang J, Yu L. Study on operating conditions of household vanadium redox flow battery energy storage system. J Energy Storage 2022;46:103859. http://dx.doi.org/10.1016/j.est.2021.103859.

[45] Yan H, Zhang D, Qilu, Duo X, Sheng X. A review of spinel lithium titanate (Li4Ti5O12) as electrode material for advanced energy storage devices. Ceram Int 2021;47(5):5870–95. http://dx.doi.org/10.1016/j.ceramint.2020.10.241.

[46] Lourenssen K, Williams J, Ahmadpour F, Clemmer R, Tasnim S. Vanadium redox flow batteries: A comprehensive review. J Energy Storage 2019;25:100844. http://dx.doi.org/10.1016/j.est.2019.100844.

[47] Xiaohe Y, Chenghong G, Xin Z, Furong L. Robust optimization-based energy storage operation for system congestion management. IEEE Syst J 2020;14:2694–702. http://dx.doi.org/10.1109/JSYST.2019.2932897.

[48] Alharbi W, Almutairi A. Planning flexibility with non-deferrable loads considering distribution grid limitations. IEEE Access 2021;9:25140–7. http://dx.doi.org/10.1109/ACCESS.2021.3057553.

[49] Trivedi A, Aih HC, Srinivasan D. A stochastic cost-benefit analysis framework for allocating energy storage system in distribution network for load leveling. Appl Energy 2020;280:115944. http://dx.doi.org/10.1016/j.apenergy.2020.115944.

[50] Chadly A, Azar E, Maalouf M, Mayyas A. Techno-economic analysis of energy storage systems using reversible fuel cells and rechargeable batteries in green buildings. Energy 2022;247:123466. http://dx.doi.org/10.1016/j.energy.2022.123466.

[51] Lima LS, Quartier M, Buchmayr A, Sanjuan-Delm'as D, Laget H, Corbisier D, et al. Life cycle assessment of lithium-ion batteries and vanadium redox flow batteries-based renewable energy storage systems. Sustain Energy Technol Assess 2021;46:101286. http://dx.doi.org/10.1016/j.seta.2021.101286.

[52] Rivera FP, Zalamea J, Espinoza JL, Gonzalez LG. Sustainable use of spilled turbinable energy in Ecuador: Three different energy storage systems. Renew Sustain Energy Rev 2022;156:112005. http://dx.doi.org/10.1016/j.rser.2021.112005.

[53] Garcia-Torres F, Bordons C, Tobajas J, Real-Calvo R, Santiago I, Grieu S. Stochastic optimization of microgrids with hybrid energy storage systems for grid flexibility services considering energy forecast uncertainties. IEEE Trans Power Syst 2021;36(6):5537–47. http://dx.doi.org/10.1109/TPWRS.2021.3071867.

[54] Cao W, Xiao J, Cui S, Liu X. An efficient and economical storage and energy sharing model for multiple multi-energy microgrids. Energy 2022;244:123124. http://dx.doi.org/10.1016/j.energy.2022.123124.

[55] Diab A, Sultan H, Mohamed I, Kuznetsov O, Do T. Application of different optimization algorithms for optimal sizing of PV/Wind/Diesel/Battery storage stand-alone hybrid microgrid. IEEE Access 2019;7:119223–45. http://dx.doi.org/10.1109/ACCESS.2019.2936656.

[56] Leonori S, Paschero M, Frattale-Mascioli F, Rizzi R. Optimization strategies for Microgrid energy management systems by Genetic Algorithms. Appl Soft Comput 2020;86:105903. http://dx.doi.org/10.1016/j.asoc.2019.105903.

[57] Yu V, Le A, Jatinder Gupta J. Sustainable microgrid design with multiple demand areas and peer-to-peer energy trading involving seasonal factors and uncertainties. Renew Sustain Energy Rev 2022;161:112342. http://dx.doi.org/10.1016/j.rser.2022.112342.

[58] Khan M, Wang J, Ma M, Xiong L, Li P, Wu F. Optimal energy management and control aspects of distributed microgrid using multi-agent systems. Sustainable Cities Soc 2019;44:855–70. http://dx.doi.org/10.1016/j.scs.2018.11.009.

[59] Dong X, Li X, Cheng S. Energy management optimization of microgrid cluster based on multi-agent-system and hierarchical stackelberg game theory. IEEE Access 2020;8:206183–97. http://dx.doi.org/10.1109/ACCESS.2020.3037676.

[60] Tooryan F, HassanzadehFard H, Collins E, Jin S, Ramezani B. Optimization and energy management of distributed energy resources for a hybrid residential microgrid. J Energy Storage 2020;30:101556. http://dx.doi.org/10.1016/j.est.2020.101556.

[61] Khasanzoda N, Safaraliev M, Zicmane I, Beryozkina S, Rahimov J, Ahyoev J. Use of smart grid based wind resources in isolated power systems. Energy 2022;253:124188. http://dx.doi.org/10.1016/j.energy.2022.124188.

[62] Faisal M, Hannan MA, Ker PJ, Rahman MSA, Begum RA, Mahlia TMI. Particle swarm optimised fuzzy controller for charging–discharging and scheduling of battery energy storage system in MG applications. Energy Rep 2020;6:215–28. http://dx.doi.org/10.1016/j.egyr.2020.12.007.

[63] Indragandhi V, Logesh R, Subramaniyaswamy V, Vijayakumar V, Siarry P, et al. Multi-objective optimization and energy management in renewable based AC/DC microgrid. Comput Electr Eng 2018;70:179–98. http://dx.doi.org/10.1016/j.compeleceng.2018.01.023.

[64] Haidar A, Fakhar A, Helwig A. Sustainable energy planning for cost minimization of autonomous hybrid microgrid using combined multi-objective optimization algorithm. Sustainable Cities Soc 2020;62:102391. http://dx.doi.org/10.1016/j.scs.2020.102391.

[65] Kharrich M, Mohammed O, Alshammari N, Akherraz M. Multi-objective optimization and the effect of the economic factors on the design of the microgrid hybrid system. Sustainable Cities Soc 2021;65:102646. http://dx.doi.org/10.1016/j.scs.2020.102646.

[66] Eskandari H, Kiani M, Zadehbagheri M, Niknam T. Optimal scheduling of storage device, renewable resources and hydrogen storage in combined heat and power microgrids in the presence plug-in hybrid electric vehicles and their charging demand. J Energy Storage 2022;50:104558. http://dx.doi.org/10.1016/j.est.2022.104558.

[67] Khosravi N, Echalih S, Baghbanzadeh R, Hekss Z, Hassani R, Messaoudi M. Enhancement of power quality issues for a hybrid AC/DC microgrid based on optimization methods. IET Renew Power Gener 2022;16(8):1773–91. http://dx.doi.org/10.1049/rpg2.12476.

[68] Shukla S, Pandit M. An optimum multi-objective dynamic scheduling strategy for a hybrid microgrid system using fuzzy rank-based modified differential evolution algorithm. In: Artificial intelligence and sustainable computing. Singapore: Springer Singapore; 2022, p. 175–88.

[69] Marcelino C, Almeida P, Wanner E, Baumann M, Weil M, Carvalho L, et al. Solving security constrained optimal power flow problems: a hybrid evolutionary approach.. Appl Intell 2018;48:3672–90. http://dx.doi.org/10.1007/s10489-018-1167-5.

[70] Borhanazad H, Mekhilef S, Gounder-Ganapathy V, Modiri-Delshad M, Ali M. Optimization of micro-grid system using MOPSO. Renew Energy 2014;71:295–306. http://dx.doi.org/10.1016/j.renene.2014.05.006.

[71] Ramli MAM, Bouchekara HREH, Alghamdi AS. Optimal sizing of PV/wind/diesel hybrid microgrid system using multi-objective self-adaptive differential evolution algorithm. Renew Energy 2018;121:400–11. http://dx.doi.org/10.1016/j.renene.2018.01.058.

[72] Abuelrub A, Khamees M, Ababneh J, Al-Masri H. Hybrid energy system design using greedy particle swarm and biogeography-based optimisation. IET Renew Power Gener 2020;14:1657–67. http://dx.doi.org/10.1049/iet-rpg.2019.0858.

[73] Marcelino C, Baumann M, Carvalho L, Chibeles-Martins N, Wanner E, Almeida P, et al. A Combined Optimization and Decision Making Approach for Battery Supported HMGS. J Oper Res Soc 2020;71:762–74. http://dx.doi.org/10.1080/01605682.2019.1582590.

[74] Eichfelder G. Scalarization approaches. in: adaptive scalarization methods in multiobjective optimization, vol. 1. Berlin, Heidelberg.: Springer; 2008, p. 21–6. http://dx.doi.org/10.1007/978-3-540-79159-1_2.

[75] Hughes L, Bell J. Compensating customer-generators: a taxonomy describing methods of compensating customer-generators for electricity supplied to the grid. Energy Policy 2006;34(13):1532–9.

[76] Poullikkas A, Kourtis G, Hadjipaschalis I. A review of net metering mechanism for electricity renewable energy sources. Int J Energy Environ (Print) 2013;4.

[77] Darghouth NR, Barbose G, Wiser R. The impact of rate design and net metering on the bill savings from distributed PV for residential customers in california. Energy Policy 2011;39(9):5243–53.

[78] Kyritsis A, Roman E, Kalogirou SA, Nikoletatos J, Agathokleous R, Mathas E, et al. Households with fibre reinforced composite BIPV modules in southern Europe under net metering scheme. Renew Energy 2019;137:167–76.

[79] Zehir MA, Batman A, Sonmez MA, Font A, Tsiamitros D, Stimoniaris D, et al. Impacts of microgrids with renewables on secondary distribution networks. Appl Energy 2017;201:308–19.

[80] SODA. Solar radiation and meteorological data services to optimize solar energy production toward a sustainable future. 2022, https://www.soda-pro.com/ Available in 16th march 2022.

[81] Mallol-Poyato R, Jimenez-Fernandez S, Diaz-Villar D, Salcedo-Sanz S. Joint optimization of a microgrid's structure design and its operation using a two-steps evolutionary algorithm. Energy 2016;94:775–85. http://dx.doi.org/10.1016/j.energy.2015.11.030.

[82] Baumann M, Peters J, Weil M, Grunwald A. CO2 Footprintand Life-Cycle Costsof ElectrochemicalEnergyStoragefor StationaryGridApplications. Energy Technol 2017;5:1071–83. http://dx.doi.org/10.1002/ente.201600622.

[83] Baumann M, Peters J, Weil M, Marcelino C, Almeida P, Wanner E. Environmental impacts of different battery technologies in renewable hybrid micro-grids. In: 2017 IEEE PES innovative smart grid technologies conference Europe (ISGT-Europe). 2017, p. 1–6. http://dx.doi.org/10.1109/ISGTEurope.2017.8260137.

[84] Ibrahim H, Ilinca A, Perron J. Energy storage systems-Characteristics and comparisons. Renew Sustain Energy Rev 2008;12(5):1221–50. http://dx.doi.org/10.1016/j.rser.2007.01.023.

[85] Chen H, Cong T, Yang W, Tan C, Li Y, Ding Y. Progress in electrical energy storage system: A critical review. Progr. Nat. Sci. 2009;19(3):291–312. http://dx.doi.org/10.1016/j.pnsc.2008.07.014.

[86] Arbabzadeh M, Johnson J, keoleian G, Rasmussen P, Thompson L. Twelve principles for green energy storage in grid applications. Environ Sci Technol 2016;50(2):1046–55. http://dx.doi.org/10.1021/acs.est.5b03867.

[87] Arenas L, León C, Walsh F. Engineering aspects of the design, construction and performance of modular redox flow batteries for energy storage. J Energy Storage 2017;11:119–53. http://dx.doi.org/10.1016/j.est.2017.02.007.

[88] Weber S, Peters J, Baumann M, weil M. Life Cycle Assessment of a Vanadium Redox Flow Battery. Environ Sci Technol 2018;52:10864–73. http://dx.doi.org/10.1021/acs.est.8b02073.

[89] Faisal M, Hannan M, Ker P, Hussain A, Mansor M, Blaabjerg F. Review of energy storage system technologies in microgrid applications: Issues and challenges. IEEE Access 2018;6:35143–64. http://dx.doi.org/10.1109/ACCESS.2018.2841407.

[90] Guo Z, Liu Z, Sun X, Du T, Zhang D, An Y, et al. Probing current contribution of lithium-ion battery/lithium-ion capacitor multi-structure hybrid systems. J Power Sources 2022;548:232016. http://dx.doi.org/10.1016/j.jpowsour.2022.232016.

[91] Graditi G, Ippolito M, Telaretti E, Zizzo G. Technical and economical assessment of distributed electrochemical storages for load shifting applications: An Italian case study. Renew Sustain Energy Rev 2016;57:515–23. http://dx.doi.org/10.1016/j.rser.2015.12.195.

[92] Stenzel P, Baumann M, Fleer J, Zimmermann B, Weil M. Database development and evaluation for techno-economic assessments of electrochemical energy storage systems. In: 2014 IEEE International energy conference. ENERGYCON, 2014, p. 1334–42. http://dx.doi.org/10.1109/ENERGYCON.2014.6850596.

[93] Carvalho L, da Silva A, Miranda V. Security-constrained optimal power flow via cross-entropy method. IEEE Trans Power Syst 2018;33:6621–9. http://dx.doi.org/10.1109/TPWRS.2018.2847766.

[94] Camacho-Gomez C, Jimenez-Fernandez S, Mallol-Poyato R, Del-Ser J, Salcedo-Sanz S. Optimal design of Microgrid's network topology and location of the distributed renewable energy resources using the Harmony Search algorithm. Soft Comput 2019;23:6495–510. http://dx.doi.org/10.1007/s00500-018-3300-0.

[95] Martínez-Rodríguez D, Colmenar J, Hidalgo J, Villanueva R-J, Salcedo-Sanz S. Particle swarm grammatical evolution for energy demand estimation. Energy Sci Eng 2020;8(4):1068–79. http://dx.doi.org/10.1002/ese3.568.

[96] Storn R, Price K. Differential evolution - A simple and efficient heuristic for global optimization over continuous spaces. J Global Optim 1997;11:341–59.

[97] Kennedy J, Eberhart R. Particle swarm optimization. In: Proceedings of ICNN'95 - International conference on neural networks, vol. 4. 1995, p. 1942–8 vol.4. http://dx.doi.org/10.1109/ICNN.1995.488968.

[98] Marcelino C, G. Leite C, Delgado, L. Oliveira EW, Jimenes-Fernandez S, Salcedo-Sanz S. An efficient multi-objective evolutionary approach for solving the operation of multi-reservoir system scheduling in hydro-power plants. Expert Syst Appl 2021;185:115638. http://dx.doi.org/10.1016/j.eswa.2021.115638.

[99] Wasserstein RL, Lazar NA. The ASA statement on p-values: Context, process, and purpose. Amer Statist 2016;70:129–33. http://dx.doi.org/10.1080/00031305.2016.1154108.

[100] Conover WJ. Practical nonparametric statistics, vol. 350. John Wiley & Sons; 1999.

[101] Holm S. A simple sequentially rejective multiple test procedure. Scand J Stat 1979;6:65–70, URL http://www.jstor.org/stable/4615733.